

**APPENDIX G**

**UNCERTAINTY IN FLOW PATH LENGTHS IN TUFF AND ALLUVIUM  
(RESPONSE TO RT 2.08, RT 3.03, AND USFIC 5.04)**

### **Note Regarding the Status of Supporting Technical Information**

This document was prepared using the most current information available at the time of its development. This Technical Basis Document and its appendices providing Key Technical Issue Agreement responses that were prepared using preliminary or draft information reflect the status of the Yucca Mountain Project's scientific and design bases at the time of submittal. In some cases this involved the use of draft Analysis and Model Reports (AMRs) and other draft references whose contents may change with time. Information that evolves through subsequent revisions of the AMRs and other references will be reflected in the License Application (LA) as the approved analyses of record at the time of LA submittal. Consequently, the Project will not routinely update either this Technical Basis Document or its Key Technical Issue Agreement appendices to reflect changes in the supporting references prior to submittal of the LA.

## APPENDIX G

### UNCERTAINTY IN FLOW PATH LENGTHS IN TUFF AND ALLUVIUM (RESPONSE TO RT 2.08, RT 3.03, AND USFIC 5.04)

This appendix provides a response for Key Technical Issue (KTI) agreements Radionuclide Transport (RT) 2.08, RT 3.03, and Unsaturated and Saturated Flow Under Isothermal Conditions (USFIC) 5.04. These KTI agreements relate to providing additional information about flow path uncertainties in the alluvium and tuff.

#### G.1 KEY TECHNICAL ISSUE AGREEMENTS

##### G.1.1 RT 2.08, RT 3.03, and USFIC 5.04 Agreements

KTI agreements RT 2.08 and RT 3.03 were reached during the U.S. Nuclear Regulatory Commission (NRC)/U.S. Department of Energy (DOE) technical exchange and management meeting on radionuclide transport held December 5 through 7, 2000, in Berkeley, California. Radionuclide transport KTI subissues 1, 2 and 3 were discussed at that meeting (Reamer and Williams 2000a).

KTI agreement USFIC 5.04 was reached during the NRC/DOE technical exchange and management meeting on unsaturated and saturated flow under isothermal conditions held October 31 through November 2, 2000, in Albuquerque, New Mexico. The saturated zone portion of KTI subissues 5 and 6 was discussed at that meeting (Reamer and Williams 2000b).

Wording of these agreements is:

##### RT 2.08

Provide additional information to further justify the uncertainty distribution of flow path lengths in the alluvium. This information currently resides in the Uncertainty Distribution for Stochastic Parameters Analysis and Model Report (AMR). DOE will provide additional information, to include Nye County data as available, to further justify the uncertainty distribution of flowpath lengths in alluvium in updates to the Uncertainty Distribution for Stochastic Parameters AMR and to the Saturated Zone Flow and Transport Process Model Report, both expected to be available in FY 2002.

##### RT 3.03

Provide additional information to further justify the uncertainty distribution of flow path lengths in the tuff. This information currently resides in the Uncertainty Distribution for Stochastic Parameters AMR. DOE will provide additional information, to include Nye County data as available, to further justify the uncertainty distribution of flowpath lengths from the tuff at the water table through the alluvium at the compliance boundary in updates to the Uncertainty Distribution for Stochastic Parameters AMR and to the Saturated Zone Flow and Transport Process Model Report, both expected to be available in FY 2002.

## **USFIC 5.04**

Provide additional information to further justify the uncertainty distribution of flow path lengths in the alluvium. This information currently resides in the Uncertainty Distribution for Stochastic Parameters AMR. DOE will provide additional information, to include Nye County data as available, to further justify the uncertainty distribution of flowpath lengths in alluvium in updates to the Uncertainty Distribution for Stochastic Parameters AMR and to the Saturated Zone Flow and Transport PMR, both expected to be available in FY 2002.

### **G.1.2 Related Key Technical Issue Agreements**

RT 2.08, RT 3.03, and USFIC 5.04 all pertain to questions regarding flow paths. RT 3.03 only differs in that it discusses flow paths in tuff rather than alluvium. All three agreements are addressed in this appendix.

## **G.2 RELEVANCE TO REPOSITORY PERFORMANCE**

The subject of these agreements is the further definition of flow-path length uncertainty in the tuffs and alluvium. This is directly relevant to the uncertainty of saturated zone flow and transport model output and, subsequently, to performance assessment. Characterization of the flow paths, including uncertainty, comprises part of the characterization work and a description of the hydrology. Flow paths are part of the output of the saturated zone flow and transport model, therefore, directly affect performance assessment.

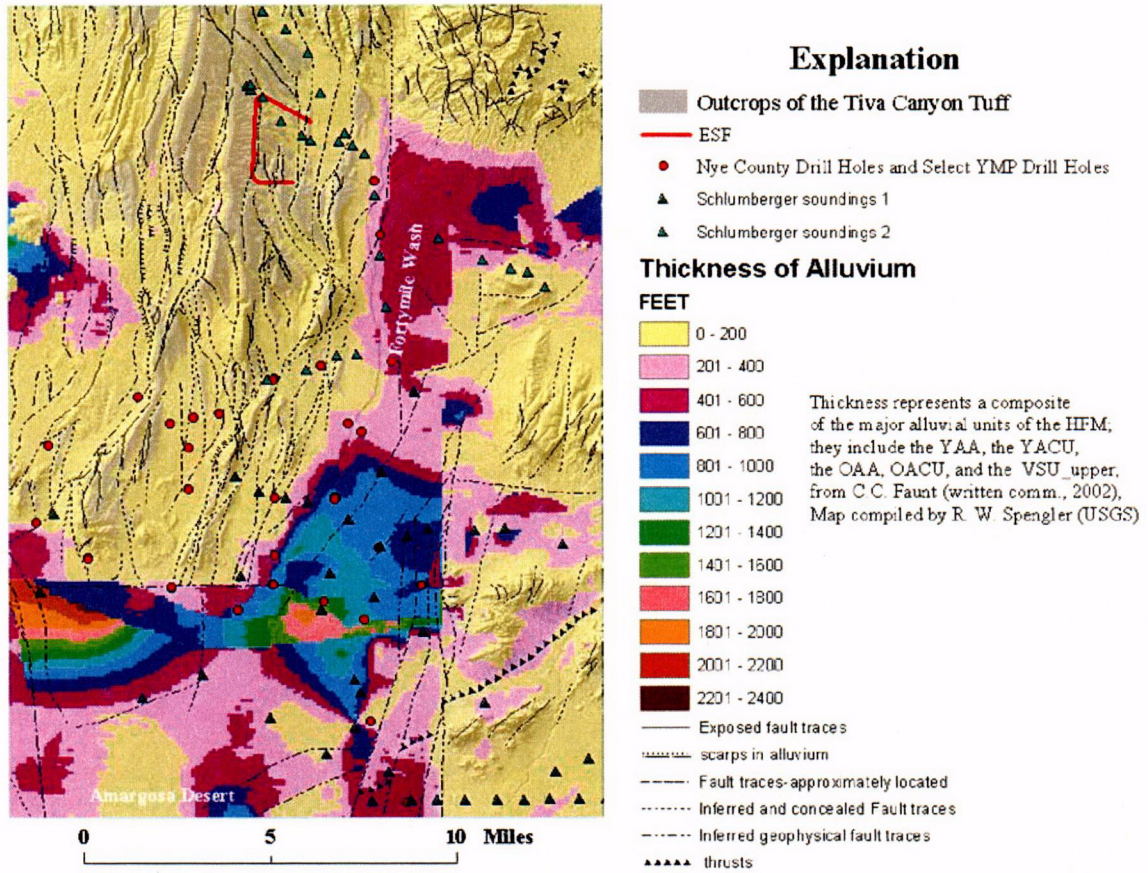
Groundwater flow path lengths in the saturated zone to the accessible environment affect the potential transport of radionuclides. Because the flow paths are close to the water table and transition from the volcanic tuffs to the alluvium, flow-path uncertainty directly affects the length of flow in the volcanic tuffs and in the alluvium. In particular, the relative lengths of the flow path in the tuff and the alluvium may have a large effect on the transport times of potential radionuclides through the saturated zone system because of different transport characteristics in the two media. The tuff aquifer is a fractured medium in which groundwater flow is limited to the fracture network, and access to the rock matrix porosity depends on the relatively slow process of matrix diffusion. The alluvium aquifer is a porous medium in which the groundwater flow is more widely distributed and groundwater velocities are slower relative to the tuff aquifer. In addition, the sorption coefficient for some radionuclides (e.g.,  $^{237}\text{Np}$ ) may be higher in alluvium than in the tuff matrix, leading to longer transport times in the alluvium relative to the tuff aquifer.

Additional discussion related to this subject is provided in Section 3.

### **G.3 RESPONSE**

Uncertainty in the length of the saturated zone flow paths in tuff and alluvium is related to uncertainties in two underlying characteristics of the saturated zone system. First, there is uncertainty in the contact location between the tuff and the alluvium. Second, there is uncertainty in the specific groundwater flow directions and the resulting flow pathways from beneath the repository to the accessible environment. Interaction between these two sources of

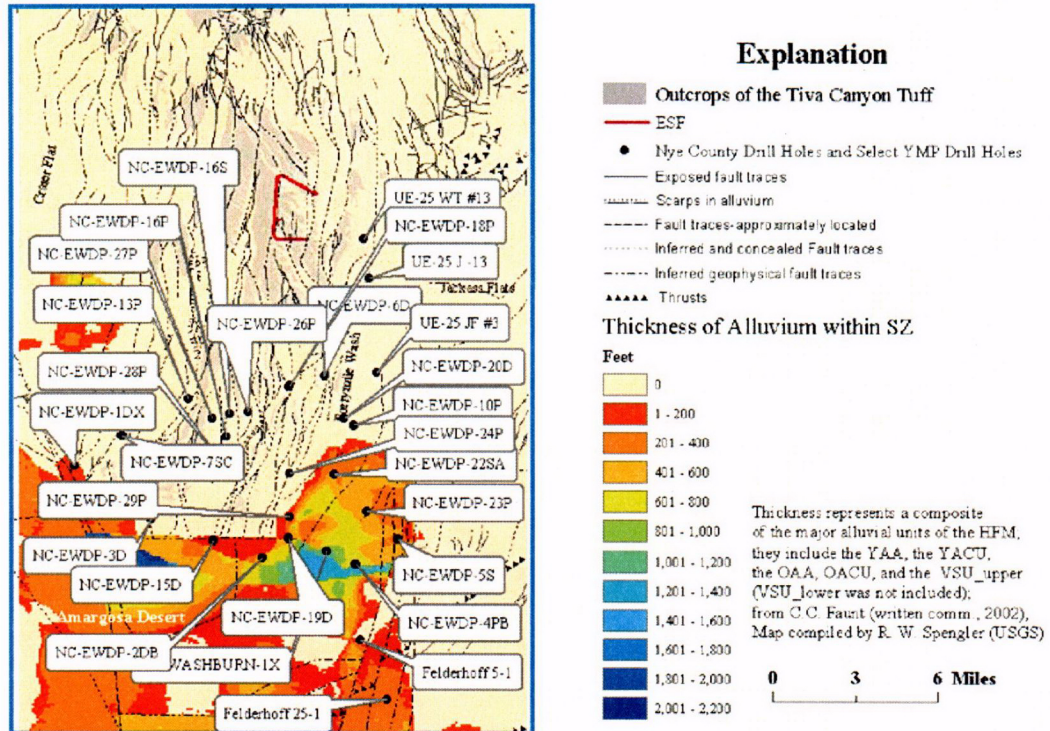
uncertainty accounts for the overall uncertainty in the flow path lengths in the tuff and alluvium. Uncertainty in the subsurface geology has been reduced in the area near the contact between the tuff and alluvium at the water table by wells in the Nye County Early Warning Drilling Program (Figure G-1a and G-1b). Figure G-1b shows saturated alluvium thickness. Lithologic and water-level data from wells have been used to constrain the uncertainty in the location at which groundwater flow moves from the tuff to the alluvium. Uncertainty in flow paths through the tuff aquifer has been evaluated through analyses and quantification of uncertainty in the horizontal anisotropy of permeability (Appendix E). These analyses are based on reevaluation of pumping test data from the C-Wells complex (BSC 2003a).



00346DCb\_011.ai

Source: DTN: GS021008312332.002.

Figure G-1a. Thickness of Alluvial Deposits in the Vicinity of Yucca Mountain



00346DCb\_012.ai

Source: DTN: GS021008312332.002.

Figure G-1b. Saturated Thickness of Alluvial Deposits in the Vicinity of Yucca Mountain

The total flow path length from beneath the repository to the compliance boundary varies from about 19.5 to 22 km, depending on the source location beneath the repository and the horizontal anisotropy in permeability in the volcanic units (BSC 2003b, Table 6-7). Uncertainty in the length of the flow path in the alluvium varies from about 10 to 1 km, also depending on the source location beneath the repository, the horizontal anisotropy in permeability in the volcanic units, and the location of the western boundary of the alluvium uncertainty zone (BSC 2003b, Table 6-7). The technical basis for the uncertainty in flow path lengths in tuff and alluvium is currently provided in *SZ Flow and Transport Model Abstraction* (BSC 2003b). Technical discussions on this subject, originally presented in *Uncertainty Distribution for Stochastic Parameters* (CRWMS M&O 2000), have been incorporated into *SZ Flow and Transport Model Abstraction* (BSC 2003b).

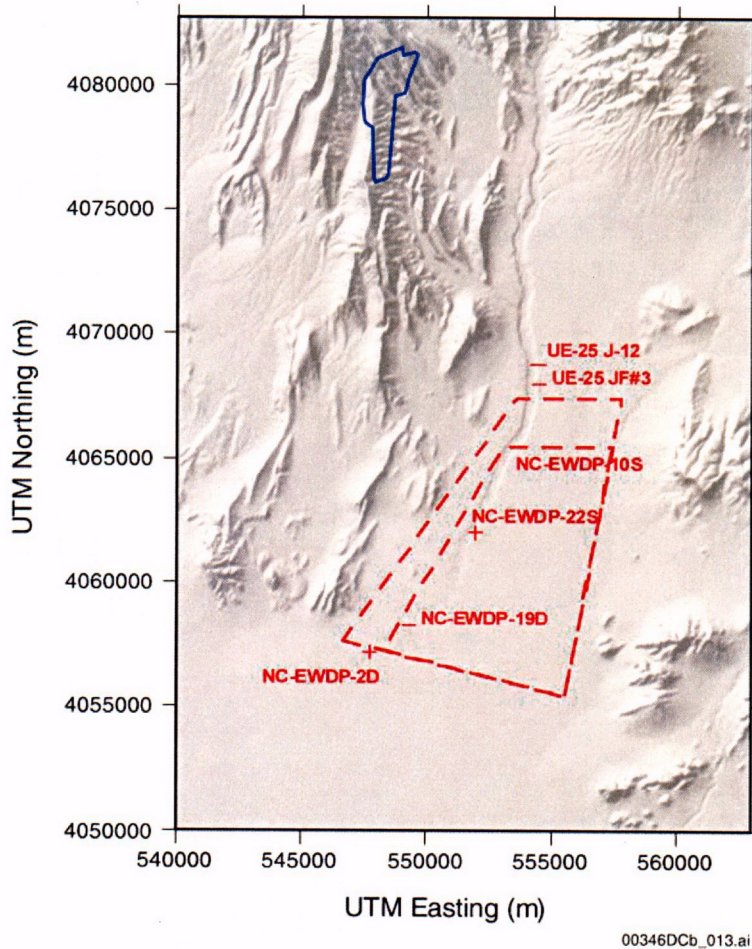
The information in this report is responsive to agreements RT 2.08, RT 3.03, and USFIC 5.04 made between the DOE and NRC. The report contains the information that DOE considers necessary for the NRC to review for closure of these agreements.

## G.4 BASIS FOR THE RESPONSE

### G.4.1 Hydrogeologic Uncertainty

Uncertainty in the geology below the water table exists along the inferred flow path from the repository at distances of approximately 10 to 20 km downgradient of the repository. The

uncertainty in the northerly and westerly extent of the alluvium in the saturated zone of the site-scale flow and transport system is abstracted as a polygonal region that is assigned radionuclide transport properties representative of the valley-fill aquifer hydrogeologic unit (alluvium). The dimensions of the polygonal region are randomly varied in *SZ Flow and Transport Model Abstraction* (BSC 2003b) for the multiple realizations used in probabilistic assessment of uncertainty. The northern boundary of the uncertainty zone is varied between the dashed lines at the northern end of the polygonal area shown in Figure G-2. The western boundary of the uncertainty zone is varied between the dashed lines along the western side of the polygonal area shown in the Figure G-2.



Sources: Repository outline: BSC 2003c; alluvial uncertainty zone: BSC 2003b; well locations: DTN: GS010908312332.002.

NOTE: Repository outline is shown by the solid line and the minimum and maximum boundaries of the alluvium uncertainty zone are shown by the dashed lines. Key well locations and well numbers are shown with the cross symbols.

Figure G-2. Minimum and Maximum Extent of the Alluvium Uncertainty Zone

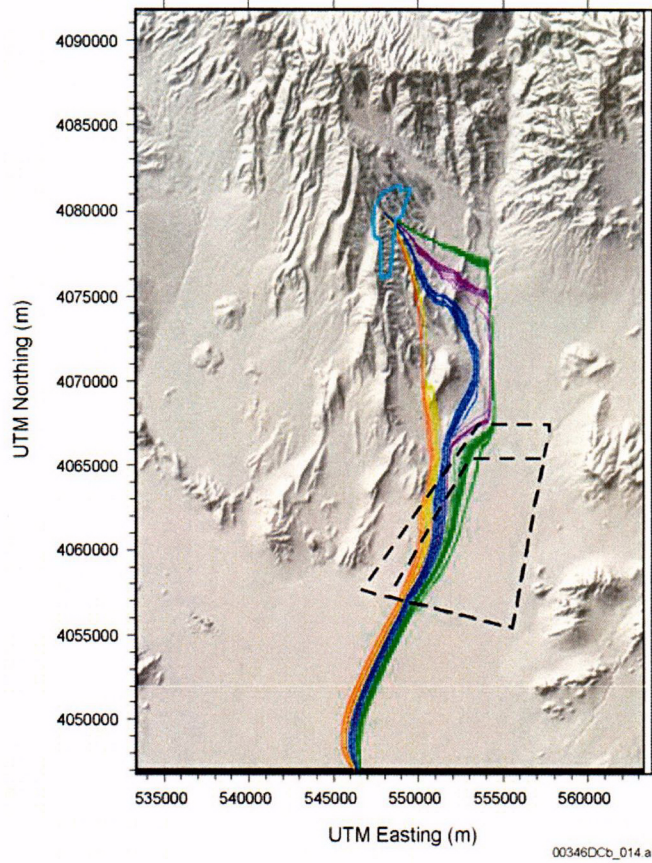
Uncertainty in the contact between volcanic rocks and alluvium at the water table along the northern part of the uncertainty zone is approximately bounded by the location of well UE-25 JF#3, in which the water table is below the contact between the volcanic rocks and the overlying

alluvium, and by the location of well NC-EWDP-10S, in which the water table is above the contact between the volcanic rocks and the alluvium (Figure G-2). Uncertainty in the contact along the western part of the uncertainty zone is defined by the locations of wells NC-EWDP-10S, NC-EWDP-22S, and NC-EWDP-19D, in which the water table is above the contact between volcanic rocks and the overlying alluvium, and outcrops of volcanic bedrock to the west.

#### **G.4.2 Flow Path Uncertainty**

Uncertainty in flow paths is affected by anisotropy in hydraulic properties of the volcanic tuffs. Large-scale anisotropy and heterogeneity were implemented in the saturated zone site-scale flow model through incorporation of known hydraulic features, faults, and fractures. Small-scale anisotropy was derived from analysis of hydraulic testing at the C-Wells complex (BSC 2003a, Section 6.2.6; see also Appendix E).

There is a notable variation in the simulated saturated zone flow paths (BSC 2003b) over the range of uncertainty in the horizontal anisotropy in permeability considered in that model. The uncertainty distribution for horizontal anisotropy assigns 90 percent probability to a value of greater than 1 for the ratio of north south to east west permeability. Consequently, the most likely flow paths are to the west of the blue particle paths (Figure G-3). Figures G-4 and G-5, for comparison, show flow trajectories from the approximate footprint of the repository in the north to the 18-km compliance boundary in the south (18 km is the direct distance from the repository to the compliance boundary). The flow path length may be longer because the flow path is affected by anisotropy and the radionuclide source location. The trajectories are predicted for two calibration cases using the Center for Nuclear Waste Regulatory Analyses three-dimensional site-scale model as described by Winterle et al. (2003).



Source: Repository outline: BSC 2003c; alluvial uncertainty zone: BSC 2003b

NOTE: Green, purple, blue, yellow, and red lines show simulated particle paths for horizontal anisotropy values of 0.05, 0.20, 1.0, 5.0, and 20.0, respectively. The dashed lines show the minimum and maximum boundaries of the alluvial uncertainty zone.

Figure G-3. Simulated Particle Paths for Different Values of Horizontal Anisotropy in Permeability



00346DCb\_015.ai

Source: Winterle et al. 2003, Figure 4.

Figure G-4 Case 1 Predicted Flow Trajectories from the Approximate Footprint of the Repository in the North to the 18-km Compliance Boundary in the South



00346DCb\_016 ai

Source: Winterle et al. 2003, Figure 8

Figure G-5. Case 2 Predicted Flow Trajectories from the Approximate Footprint of the Repository in the North to the 18-km Compliance Boundary in the South

#### G.4.3 Aggregate Uncertainty in Flow Path Lengths in the Tuff and Alluvium

The effects of uncertainty in flow path lengths are evaluated in the saturated zone flow and transport abstraction model (BSC 2003b) in an aggregate sense. In addition, the flow path lengths are estimated for implementation in the saturated zone one-dimensional transport model (BSC 2003b). Factors influencing the flow path lengths in the tuff and alluvium are the source location at the water table beneath the repository, the horizontal anisotropy, and the location of the contact between tuff and alluvium at the water table. Except for some values of the horizontal anisotropy ratio of less than 1, the uncertainty in the simulated flow path length in the alluvium is only a function of the location of the western boundary of the alluvial uncertainty zone (Figure G-3). Uncertainty in the northern location of the contact between the tuff and alluvium at the water table has been reduced by lithologic information from wells NC-EWDP-10S and NC-EWDP-22S. However, sufficient uncertainty remains regarding the western location of the contact between the tuff and alluvium to effect uncertainty in the flow path lengths in the alluvium.

The total flow path lengths from beneath the repository to the compliance boundary vary from about 19.5 to 22 km, depending on the source location beneath the repository and the horizontal

anisotropy in permeability in the volcanic units (BSC 2003b, Table 6-7). Uncertainty in the flow path length in the alluvium varies from about 1 to 10 km, also depending on the source location beneath the repository, the horizontal anisotropy in permeability in the volcanic units, and the location of the western boundary of the alluvium uncertainty zone (BSC 2003b, Table 6-7).

The evaluation of uncertainty of flow path lengths in tuff and alluvium has been incorporated into the saturated zone transport model for license application by identifying an alluvium uncertainty zone and then abstracted as a polygonal region that is assigned radionuclide transport properties representative of the valley-fill aquifer hydrogeologic unit (alluvium). The dimensions of the polygonal region (shown in Figure G-2) are randomly varied in the *SZ Flow and Transport Model Abstraction* (BSC 2003b) for the multiple realizations used in probabilistic assessment of uncertainty, which allows for the range of uncertainty to be reflected in the results. The flow-path lengths in the alluvium and fracture tuffs are justified using field data and analyses. Uncertainty associated with the flow path lengths is propagated to the total system performance assessment for the license application assessments.

## G.5 REFERENCES

### G.5.1 Documents Cited

BSC (Bechtel SAIC Company) 2003a. *Saturated Zone In-Situ Testing*. ANL-NBS-HS-000039 REV 00A. Las Vegas, Nevada: Bechtel SAIC Company. ACC: MOL.20030602.0291.

BSC 2003b. *SZ Flow and Transport Model Abstraction*. MDL-NBS-HS-000021 REV 00A. Las Vegas, Nevada: Bechtel SAIC Company. ACC: MOL.20030612.0138.

BSC 2003c. *Repository Design, Repository/PA IED Subsurface Facilities*. 800-IED-EBS0-00401-000-00C. Las Vegas, Nevada: Bechtel SAIC Company. ACC: ENG.20030303.0002.

CRWMS M&O (Civilian Radioactive Waste Management System Management and Operating Contractor) 2000. *Uncertainty Distribution for Stochastic Parameters*. ANL-NBS-MD-000011 REV 00. Las Vegas, Nevada: CRWMS M&O. ACC: MOL.20000526.0328.

Reamer, C.W. and Williams, D.R. 2000a. *Summary Highlights of NRC/DOE Technical Exchange and Management Meeting on Radionuclide Transport*. Meeting held December 5-7, 2000, Berkeley, California. Washington, D.C.: U.S. Nuclear Regulatory Commission. ACC: MOL.20010117.0063.

Reamer, C.W. and Williams, D.R. 2000b. *Summary Highlights of NRC/DOE Technical Exchange and Management Meeting on Unsaturated and Saturated Flow Under Isothermal Conditions*. Meeting held August 16-17, 2000, Berkeley, California. Washington, D.C.: U.S. Nuclear Regulatory Commission. ACC: MOL.20001201.0072.

Winterle, J.R.; Claisse, A.; and Arlt, H.D. 2003. "An Independent Site-Scale Groundwater Flow Model for Yucca Mountain." *Proceedings of the 10th International High-Level Radioactive Waste Management Conference (IHLRWM), March 30-April 2, 2003, Las Vegas, Nevada*. Pages 151-158. La Grange Park, Illinois: American Nuclear Society. TIC: 254559.

**G.5.2 Data, Listed by Data Tracking Number**

GS010908312332.002. Borehole Data from Water-Level Data Analysis for the Saturated Zone Site-Scale Flow and Transport Model. Submittal date: 10/02/2001.

GS021008312332.002. Hydrogeologic Framework Model for the Saturated-Zone Site-Scale Flow and Transport Model, Version YMP\_9\_02. Submittal date: 12/09/2002.

INTENTIONALLY LEFT BLANK

**APPENDIX H**  
**TRANSPORT PROPERTIES**  
**(RESPONSE TO RT 1.05, RT 2.01, RT 2.10, GEN 1.01 (COMMENTS 28 AND 34),**  
**AND RT 2.03 AIN-1)**

### **Note Regarding the Status of Supporting Technical Information**

This document was prepared using the most current information available at the time of its development. This Technical Basis Document and its appendices providing Key Technical Issue Agreement responses that were prepared using preliminary or draft information reflect the status of the Yucca Mountain Project's scientific and design bases at the time of submittal. In some cases this involved the use of draft Analysis and Model Reports (AMRs) and other draft references whose contents may change with time. Information that evolves through subsequent revisions of the AMRs and other references will be reflected in the License Application (LA) as the approved analyses of record at the time of LA submittal. Consequently, the Project will not routinely update either this Technical Basis Document or its Key Technical Issue Agreement appendices to reflect changes in the supporting references prior to submittal of the LA.

**APPENDIX H**  
**TRANSPORT PROPERTIES**  
**(RESPONSE TO RT 1.05, RT 2.01, RT 2.10, GEN 1.01 (COMMENTS 28 AND 34),**  
**AND RT 2.03 AIN-1)**

This appendix provides a response for Key Technical Issue (KTI) agreements Radionuclide Transport (RT) 1.05, RT 2.01, RT 2.10, General Agreement (GEN) 1.01, Comments 28 and 34, and a U.S. Nuclear Regulatory Commission (NRC) additional information needed (AIN) request for KTI agreement RT 2.03. These KTI agreements relate to providing more information justifying transport properties for the parameters derived.

## **H.1 KEY TECHNICAL ISSUE AGREEMENTS**

### **H.1.1 RT 1.05, RT 2.01, RT 2.10, GEN 1.01 (Comments 28 and 34), and RT 2.03 AIN-1**

KTI agreements RT 1.05, RT 2.01, RT 2.03, and RT 2.10 were reached during the NRC/U.S. Department of Energy (DOE) technical exchange and management meeting on radionuclide transport held December 5 through 7, 2000, in Berkeley, California. Radionuclide transport KTI subissues 1, 2 and 3 were discussed at that meeting (Reamer and Williams 2000).

A letter report responding to agreement RT 2.03 (Ziegler 2002) was submitted. Specific additional information was requested by the NRC after the staff review of this letter report was completed, resulting in RT 2.03 AIN-1 (Schlueter 2002).

During the NRC/DOE technical exchange and management meeting on thermal operating temperatures, held September 18 through 19, 2001, the NRC provided additional comments relating to these RT KTI agreements (Reamer and Gil 2001). These comments (GEN 1.01, comments 28 and 34) relate specifically to transport properties. The DOE provided initial responses to these comments (Reamer and Gil 2001).

At the September 2001 technical exchange, the NRC stated that additional documentation was needed to enable a thorough evaluation of the use of expert judgment to obtain ranges and probabilities for transport parameters used in the total system performance assessment code. The NRC staff expressed the concern that sorption coefficient ( $K_d$ ) distributions were obtained from inadequately documented expert judgments. For transport parameters derived from expert judgments, the judgments should be conducted and documented in accordance with the guidance in NUREG-1563 (Kotra et al. 1996), as applicable. For those species for which  $K_d$ s were measured or referenced, the selected ranges of  $K_d$ s used to model transport of chemical species either through porous rock or fractures should be technically supported.

At the time of the meeting, the DOE planned to provide additional documentation to explain how transport parameters obtained from expert judgments and used for performance assessment were derived. Specifically, for alluvium properties, the DOE suggested that testing at the Alluvial Testing Complex (ATC) would help confirm the applicability of laboratory-determined transport parameters. If performed, testing at the ATC also would help verify whether the alluvial aquifer could be considered a single continuum porous medium.

As indicated by their associated comments and responses, GEN 1.01 comments 28 and 34 are addressed implicitly through the response to KTI agreements RT 1.05 and RT 2.10, which are addressed in this appendix.

The wording of these agreements and of the initial DOE response to the GEN comments is:

#### **RT 1.05**

Provide additional documentation to explain how transport parameters used for performance assessment were derived in a manner consistent with NUREG-1563, as applicable. Consistent with the less structured approach for expert judgment acknowledged in NUREG-1563 guidance and consistent with DOE procedure AP-3.10Q, DOE will document how it derived the transport parameter distributions for performance assessment, in a report expected to be available in FY 2002.

#### **RT 2.01**

Provide further justification for the range of effective porosity in alluvium, considering possible effects of contrasts in hydrologic properties of layers observed in wells along potential flow paths. DOE will use data obtained from the Nye County Drilling Program, available geophysical data, aeromagnetic data, and results from the Alluvial Testing Complex testing to justify the range of effective porosity in alluvium, considering possible effects of contrasts in hydrologic properties of layers observed in wells along potential flow paths. The justification will be provided in the Alluvial Testing Complex report due in FY 2003.

#### **RT 2.03**

Provide a detailed testing plan for alluvial testing (the ATC and Nye County Drilling Program) to reduce uncertainty (for example, the plan should give details about hydraulic and tracer tests at the well 19 complex and it should also identify locations for alluvium complex testing wells and tests and logging to be performed). NRC will review the plan and provide comments, if any, for DOE's consideration. In support and preparation for the October/November 2000 Saturated Zone meeting, DOE provided work plans for the Alluvial Testing Complex and the Nye County Drilling Program (FWP-SBD-99-002, Alluvial Tracer Testing Field Work Package, and FWP-SBD-99-001, Nye County Early Warning Drilling Program, Phase II and Alluvial Testing Complex Drilling). DOE will provide test plans of the style of the Alcove 8 plan as they become available. The plan will be amended to include laboratory testing. In addition, the NRC On Site Representative attends DOE/Nye County planning meetings and is made aware of all plans and updates to plans as they are made.

**RT 2.03 AIN-1**

The purpose of the testing is to support the development of a conceptual model of groundwater flow and radionuclide transport in saturated alluvium south of Yucca Mountain, and to quantify flow and transport parameters. The distance between wells is less than 30 meters. The parameters used in performance assessment are applied to cells 500 meters on a side. Provide the justification for the use of parameter values, determined at one scale (30 meters between drill holes of the ATC test), in the total system performance assessment model that uses a different scale.

**RT 2.10**

Provide additional documentation to explain how transport parameters used for PA were derived in a manner consistent with NUREG-1563, as applicable. Consistent with the less structured approach for expert judgment acknowledged in NUREG-1563 guidance and consistent with AP-3.10Q, DOE will document how it derived the transport distributions for performance assessment, in a report expected to be available in FY 2002.

**GEN 1.01 (Comment 28)**

The different analyses in the SSPA use different values and distributions for Np sorption. This type of inconsistency makes it difficult to compare the results of the different types of analyses and their effects on repository performance. Also, the effects of coupled thermal-hydrological-chemical effects on transport parameters are not considered.

Basis: Sections 11.3.1.5.3 and 11.3.4.5 use different values and distributions for Np sorption in the analyses presented in the SSPA. This type of inconsistency makes it difficult to compare the results of the different types of analyses and their effects on repository performance. Also, although the effects of coupled thermal-hydrological-chemical effects on permeability are considered (Section 11.3.5.4.2), the effects of the temperature on sorption parameters are not addressed directly.

These comments fall under Agreement RT 1.05.

**DOE Response to GEN 1.01 (Comment 28)**

Section 11.3.1.5.3 of SSPA Volume 1 used a single, conservative value of  $K_d$  (0.3 mL/g) for Np in illustrating the effects of drift shadow zone. Section 11.3.4.5 used a range of  $K_{ds}$  (1 to 3 mL/g) for Np-237 that was selected based on AMR UZ and SZ Transport Properties (ANL-NBS-HS-000019) Rev 00. The difference will be reconciled should any one of these analyses be carried forward into a potential LA.

With regard to sorption in the EBS, partition coefficients are anticipated to vary from those in the UZ because of the large mass of iron-based corrosion products and other materials in the waste package and in the invert. The rationale for the ranges of partition coefficients in the EBS is discussed in Section 10.3.4 with final values defined in Table 10.4.4-1 of Section 10.4.4. If sorption in the EBS is carried forward to a potential LA, rationale for selected ranges for sorption coefficients will be provided per KTI agreements RT 1.05 and RT 2.10.

#### **GEN 1.01 (Comment 34)**

If radionuclide retardation is to be modeled in the EBS, sorption coefficient distributions will need to be justified in a manner consistent with existing agreements RT 1.05 and RT 2.10. For example, non-zero  $K_d$  values for technetium and iodide have not been used previously in TSPA; any future adoption of such values, as were used in the SSPA, will require stronger technical basis.

#### **DOE Response to GEN 1.01 (Comment 34)**

DOE understands that a strong basis must be provided for sorption coefficient distributions for all radionuclides that are important to performance. If retardation in the EBS is carried forward to the potential LA, implementation of KTI agreements RT 1.05 and 2.10 will provide justification for the use of radionuclide transport parameters in the performance assessment.

#### **H.1.2 Related Key Technical Issue Agreements**

RT 1.05 and RT 2.10 are identical agreements and will both be addressed by this appendix. RT 1.05, RT 2.01, RT 2.06, RT 2.07 and RT 2.10 all relate to the alluvial testing program, although they address different aspects of the testing program. RT 2.06 and RT 2.07 are related to  $K_d$  experiments in alluvium and are addressed separately in Appendix K.

### **H.2 RELEVANCE TO REPOSITORY PERFORMANCE**

The subject of these agreements is transport properties and justification for parameters and their use in performance assessment. Appendix K focuses on agreements that relate to recent work to document  $K_d$ s (sorption coefficient, also known as distribution coefficient) in alluvium. This appendix focuses principally on  $K_d$ s in volcanic tuff because those were the transport properties that were derived using a modified expert judgment methodology. Other parameters also are addressed in this appendix, but because they are a key part of the technical basis for saturated zone performance, they are discussed in the main text.

Radionuclide delay through the saturated zone is considered in the repository performance assessment. The degree of radionuclide sorption onto mineral surfaces within the rock matrix of the tuff aquifer system and in the alluvial aquifer system is the most important process affecting the ability of the saturated zone to attenuate and delay released radionuclides. Matrix diffusion, a process whereby aqueous radionuclides diffuse from actively flowing pore spaces into the relatively stagnant pore space within the rock matrix, is another important process to be

considered because the majority of saturated pore volume in the saturated tuff aquifer system comprises relatively stagnant water within the rock matrix.

The importance of the saturated zone in total system performance is reflected in its status as a principal factor, chiefly as a component of defense in depth. Furthermore, an NRC performance assessment sensitivity analysis concluded that retardation in the saturated zone is important based on higher modeled doses that result if it is removed from the analysis (NRC 1999). In particular, neptunium retardation has been a large effect on dose (NRC 1999; Codell et al. 2001).

Additional discussion associated with this subject is presented in Sections 3.2 and 3.3.

## **H.3 RESPONSE**

### **H.3.1 Introduction**

This appendix focuses on the transport parameters that are most important to overall saturated zone performance (i.e., sorption coefficients, effective porosity, and dispersivity). In discussions of other transport parameters mentioned in this appendix including flowing interval spacing (volcanics), flowing interval porosity (volcanics), effective diffusion coefficient (for matrix diffusion in volcanics), matrix porosity (volcanics), and bulk density of volcanic matrix and alluvium, the reader is referred to other documents for details. The models are less sensitive to these parameters. The issue of parameter scaling is addressed in this appendix. Colloid transport parameters (e.g., filtration rate constants, retardation factors, and the mass fraction transporting unretarded) are addressed in *Saturated Zone Colloid Transport* (BSC 2003a). Radionuclide transport in the saturated zone is sensitive to specific discharge, but specific discharge is considered a flow parameter, not a transport parameter, so it is not discussed in this appendix.

### **H.3.2 Response to RT 1.05, RT 2.10 and GEN 1.01 (Comment 28 and 34)**

Expert judgment is used in the interpretation and synthesis of data for the purposes of defining uncertainty distributions in a manner consistent with NUREG-1563 (Kotra et al. 1996). Expert judgment is used in the consideration of factors that may influence the direct application of data to the development of uncertainty distributions in transport parameters. One consideration is the potential impact of the measurement scale relative to the scale at which the parameter is applied in the radionuclide transport models. For many parameters, variability at the small scale of measurement is greater than at the scale of a single numerical grid cell in the transport model. This result comes about because populating a large volume element (i.e., a grid cell) with spatially-distributed parameter values that are randomly sampled from statistical distributions will result in an "effective" parameter value for the entire volume element that is a "weighted average" of the individual small-scale parameters populating the element. The effective parameter values from a large number of such volume elements will tend to have less variability than the variability of the original distribution of smaller-scale parameter values. However, parameter values that inherently increase with scale, such as dispersivity (longitudinal or transverse), will not necessarily follow this behavior because variability in an absolute sense will increase as absolute parameter values increase. Another consideration is general lack-of-knowledge uncertainty, which is generally incorporated into the uncertainty distribution by extending the "tails" of the distribution. This qualitative assessment of uncertainty may extend

the distribution to parameter values that are plausible, but are not necessarily directly linked to data. Another consideration is the potential impacts of features, events, and processes on the uncertainty in parameter values. There may be features, events, and processes that are not explicitly associated with the available data, but are given consideration in defining the uncertainty distributions for transport parameters.

A detailed technical basis for sorption coefficient probability distributions for the license application is provided in *Site-Scale Saturated Zone Transport* (BSC 2003b, Attachment I) and in a revision to *Radionuclide Transport Models Under Ambient Conditions* (BSC 2003c; see DTN: LA0302AM831341.002). The attachments include discussions of the parameters that affect sorption behavior of radionuclides of interest, laboratory measurements, and the results of sorption modeling using the PHREEQC v.2.3 computer code.

Laboratory measurements were performed with samples of rock and water from the Yucca Mountain site. For some radionuclides (e.g., plutonium and thorium), laboratory measurements were augmented with laboratory measurements reported in the literature for sorption on pure silica in simple electrolytes or waters similar in composition to those from well UE-25 J-13. Pure silica is a useful surrogate for tuff in sorption coefficient determinations because Yucca Mountain tuffs contain 70 to 80 weight percent SiO<sub>2</sub>. PHREEQC v.2.3 modeling was used primarily to evaluate the effects of variations in water chemistry on sorption coefficients for americium, neptunium, plutonium, and uranium.

For alluvium, sorption coefficient distributions for neptunium and uranium were derived on the basis of laboratory measurements using alluvium and water samples from boreholes drilled during Phase 2 of the Nye County Early Warning Drilling Program (NC-EWDP-10S, NC-EWDP-19D, and NC-EWDP-22S). Laboratory measurements obtained with water samples from borehole NC-EWDP-3S were not used in the derivation of the sorption coefficient distributions for neptunium. For americium, plutonium, and cesium, sorption coefficient distributions derived for devitrified tuff were used to represent sorption coefficient distributions in alluvium. The mineralogic composition of alluvium reflects its volcanic provenance. Because alluvium tends to contain more clay and zeolite than devitrified tuff, this approach should yield conservative estimates of transport through lower measured sorption coefficients.

### **H.3.3 Response to RT 2.01**

The agreement cannot be addressed completely in the way it was originally planned prior to license application. Single-hole tracer and cross-hole hydraulic testing have been completed, and the results have been analyzed, but cross-hole tracer testing can not be completed prior to submitting the License Application. The testing is still planned and tentatively scheduled for fiscal year 2005, although it will depend on permit decisions. After the state permit to discharge was denied, the project developed an alternative approach that included reliance on expert opinion, literature values, single-hole tracer test results, and additional laboratory testing. Properties of alluvium are more thoroughly understood than are those of fractured tuffs (from studies completed at other sites), and the project has determined that the properties for alluvium are adequately characterized for their intended use (e.g., modeling). Even the results from the confirmatory tracer testing, if it had been completed at the ATC, would have added information from a single location, and that would not have considerably reduced the uncertainty. Without

the cross-hole tracer results, the project must continue to take no credit for matrix diffusion in the alluvium.

Conducting the ATC cross-hole tracer testing had been planned beginning in the second quarter of fiscal year 2002. The DOE maintained a policy of submitting permit requests to the State of Nevada Underground Injection Control and the State Water Engineer. The State of Nevada denied the Underground Injection Control permit request and rescinded the existing water withdrawal waiver. The testing described in the ATC Scientific Investigation Test Plan has been delayed pending resolution of permitting. Parameters developed from the ATC tests have been obtained from single-hole tracer tests and cross-hole hydraulic tests. The parameter values that have been obtained are single data points. These values will not be used directly in total system performance assessment; they will be used as confirmation that the ranges in the total system performance assessment are reasonable from site-specific results.

#### **H.3.4 Response to RT 2.03 AIN-1 Comment—Scaling of Field Parameters to Models**

The request for additional information addresses the practice of using saturated zone flow and transport parameter estimates derived from field-scale (30 to 100 m) tests in flow and transport simulations over larger scales.

The issue of extrapolation is complex and is being addressed in various ways. However, the long-term pump test in the Bullfrog Tuff at the C-Wells yielded flow parameter estimates over approximately 21 km<sup>2</sup>. It is conceivable that an area larger than the local spacing between boreholes could be affected by long-term pumping at the Alluvium Testing Complex. Thus, for flow parameters, field tests can yield parameter estimates at scales relevant to performance assessment.

Some of the methods that the project uses to address upscaling include:

1. For most flow and transport parameters, estimates derived from field-scale tests are not used directly in performance assessment models. Rather, performance assessment models randomly sample probability distributions in Monte Carlo fashion to obtain parameter values for individual simulations. The probability distributions are constructed from a variety of information sources (e.g., literature, expert elicitation, laboratory-scale tests, and field-scale tests). Parameter estimates from field-scale tests are used to refine the distributions and to ensure that the distributions are consistent with field observations (a parameter estimate from a field test at Yucca Mountain probably should not be an outlier of a distribution). Furthermore, most of the probability distributions tend to be conservative in that the field-derived parameters fall into the less conservative end of the distribution. This is practiced, in part, to allow for uncertainty associated with a lack of understanding of the scaling of flow and transport processes. The probability distributions also tend to be broad (often using log-normal or log-uniform distributions) for the same reason.
2. For some parameters, valuable insights into scaling are obtained by comparing laboratory- and field-scale parameter estimates. Although a straight-line extrapolation to larger scales is not necessarily advisable, extrapolation can be useful in constructing

probability distributions. For instance, extrapolating parameter estimates for matrix diffusion and colloid transport from laboratory, to field, and to larger scales tends to lead to constructing more conservative probability distributions than might be constructed if only field data were considered.

3. The use of geostatistical methods in two-dimensional and three-dimensional models helps address scaling issues associated with parameters that may be expected to have more spatial variability at repository scales than at field-test scales. These methods help refine the probability distributions and provide additional insights into scaling phenomena.

The information in this report is responsive to agreements RT 1.05, RT 2.01, RT 2.10, RT 2.03 AIN-1, and GEN 1.01 (Comments 28 and 34) made between the DOE and NRC. The report contains the information that DOE considers necessary for the NRC to review for closure of these agreements.

#### **H.4 BASIS FOR THE RESPONSE**

The evaluation of uncertainty in saturated zone transport parameters used for the performance assessment includes consideration of data from the Yucca Mountain site, data from other sites, expert judgment, and, in the case of dispersivity, formal expert elicitation. Appropriate site-specific data were used as the primary basis for the development of uncertainty distributions in transport parameters. These data were augmented with process model studies where appropriate. In some cases, data from the surrounding region were included in the evaluation. Regional data were used directly in some cases, and they were used as corroborative data in other cases.

The results of formal expert elicitation were used to define the uncertainty distributions for longitudinal and transverse dispersivity in the saturated zone transport simulations (CRWMS M&O 1998). This saturated zone expert elicitation was conducted in accordance with the guidance provided by Kotra et al. (1996).

##### **H.4.1 Sorption Coefficient Probability Distributions**

The technical basis for  $K_d$  distributions in the three major volcanic rock types (devitrified, zeolitic, and vitric) to be used in total system performance assessment is provided in *Site-Scale Saturated Zone Transport* (BSC 2003b, Attachment I) and in a revision to *Radionuclide Transport Models Under Ambient Conditions* (BSC 2003c; see DTN: LA0302AM831341.002). The technical basis includes an evaluation of the parameters that could influence the sorption behavior of the radionuclides of interest, an evaluation of the potential ranges for these parameters in the Yucca Mountain flow system, laboratory measurements of sorption coefficients, and the results of sorption modeling using the PHREEQC v.2.3 computer code.

Laboratory experiments were performed with samples of rock and water from the Yucca Mountain site. Two water compositions were used (from boreholes UE-25 J-13 and UE-25 p#1). These water compositions bracket the water compositions expected in the Yucca Mountain flow system over time. The potential effects of variations in water chemistry on sorption coefficients were further evaluated for some radionuclides (e.g., americium, neptunium, plutonium, and

uranium) with modeling studies using PHREEQC v.2.3. For sorption coefficients on volcanic rock, samples were obtained from various boreholes at Yucca Mountain. The samples used reflect a range of rock compositions (i.e., mineral abundances and compositions). For some radionuclides (e.g., plutonium and thorium), these laboratory measurements were augmented with those reported in the literature for sorption on pure silica in simple electrolytes or waters similar to UE-25 J-13 in composition. Pure silica is a useful substrate for sorption measurements because Yucca Mountain tuffs contain 70 to 80 weight percent SiO<sub>2</sub> (Broxton et. al. 1986).

Sorption coefficient probability distributions were derived for the three major volcanic rock types (devitrified, zeolitic, and vitric) using the results of laboratory measurements, computer modeling, and expert judgment. Separate distributions were derived for the unsaturated zone and the saturated zone. The differences in these distributions include effects due to differences in water compositions, mineral compositions, and radionuclide concentrations. On average, pore waters in the unsaturated zone have higher ionic strengths than waters in the saturated zone. Thus, the sorption coefficient probability distributions for the unsaturated zone were more heavily weighted toward the laboratory results and modeling studies involving UE-25 p#1 water. Secondary mineral compositions in the unsaturated zone are generally more enriched in alkaline earth elements compared to secondary minerals in the saturated zone. Therefore, the sorption coefficient probability distributions for the unsaturated zone were weighted towards the results of laboratory measurements with rock samples enriched in alkaline earth elements. Finally, radionuclide concentrations in the unsaturated zone are expected to be higher on average than the concentrations in the saturated zone. Therefore, the sorption coefficient probability distributions for the unsaturated zone are weighted towards experiments carried out at the higher radionuclide concentrations.

In the saturated zone, each total system performance assessment realization (i.e., calculation) uses a single value for the sorption coefficient of each radionuclide of interest. To incorporate the effect of variability in major mineral content in saturated zone hydrologic units, distributions of effective sorption coefficients were derived. The approach used to derive these distributions involved modeling the sorption behavior of selected radionuclides in a 500-m grid block with mineral distributions reflecting the range of mineral distributions encountered along potential flow paths to the accessible environment. These mineral distributions were combined with sorption coefficient distributions for the major rock types to obtain effective sorption coefficient distributions for the 500-m grid blocks. Breakthrough curves were obtained for the grid blocks using discrete values for sorption coefficients relative to the mineralogy of the block and using the effective sorption coefficient. The resulting breakthrough curves were nearly identical (see Figure I-6 in Appendix I).

For alluvium, sorption coefficient distributions for neptunium and uranium were derived on the basis of laboratory measurements using alluvium and water samples from boreholes NC-EWDP-10S, NC-EWDP-19D, and NC-EWDP-22S. Laboratory measurements obtained with water samples from borehole NC-EWDP-3S were not used in the derivation of the sorption coefficient distributions for neptunium because of the possibility that this water may have been contaminated by drilling operations. For americium, plutonium and cesium, sorption coefficient distributions derived for devitrified tuff were used to represent sorption coefficient distributions in alluvium. The mineralogic composition of alluvium clearly reflects its volcanic provenance.

Because alluvium tends to contain more clay and zeolite than devitrified tuff, this approach should yield conservative estimates of transport.

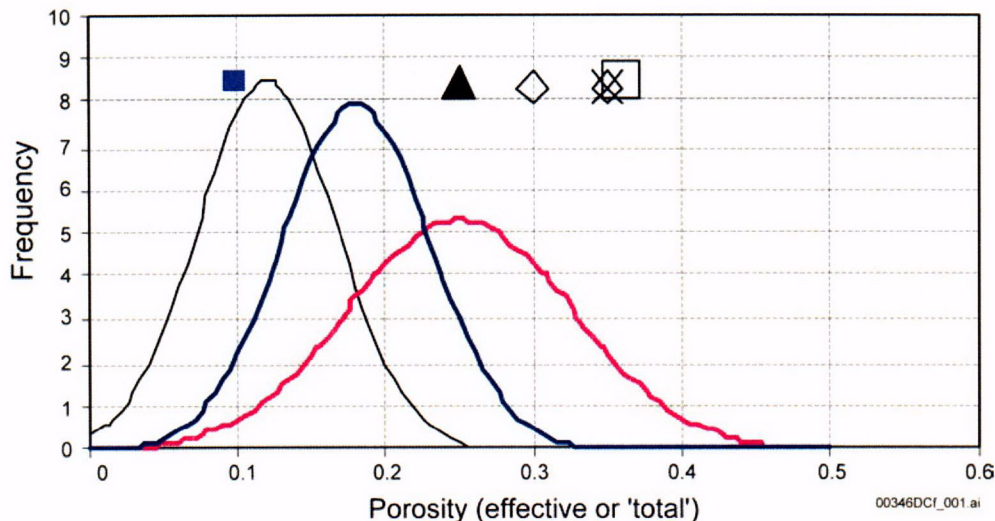
#### H.4.2 Effective Porosity of the Alluvium

A site-specific value was determined for effective porosity from borehole NC-EWDP-19D1 based on a single-well pumping test (BSC 2003d). There are total porosity values from this borehole based on borehole gravimeter surveys, which are used in developing the upper bound of the effective porosity in the alluvium uncertainty distribution.

Effective porosity is important in determining the average linear groundwater velocities used in the simulation of radionuclide transport, which is customarily calculated by dividing the specific discharge of groundwater through a model grid cell by the effective porosity,  $\phi_e$ . Groundwater velocities are more accurate when dead-end pores, and low permeability zones, which are bypassed by flow, are eliminated from consideration because they do not transmit water. As a result,  $\phi_e$  will always be less than or equal to total porosity,  $\phi_T$ . The retardation coefficient,  $R_f$ , is also a function of porosity. However, it should be a function of the total porosity within flowing pathways, which is better approximated by  $\phi_T$  than by  $\phi_e$ .

Effective porosity is treated as an uncertain parameter for the two alluvium hydrogeologic units in the site-scale saturated zone flow model (SSFM). Uncertain, in this sense, means that  $\phi_e$  will be constant spatially for each unit for any particular model realization, but that value will vary from one realization to the next. In comparison, constant parameters are constant spatially and do not change from realization to realization.

The effective porosity uncertainty distribution used for total system performance assessment for the site recommendation is shown in Figure H-1. Figure H-1 shows the distribution of Bedinger et al. (1989) and the distributions, ranges, and values from the other sources that were considered when developing the uncertainty distribution. The site-specific effective porosity value for borehole NC-EWDP-19D1, 0.1 (BSC 2003d, Section 6.5), is shown on Figure H-1. This corroborative data point falls within the uncertainty distribution.



Source: BSC 2003e, Figure 6-8.

NOTE: The single value data points do not have a y-scale value, but do correspond to the x-axis. These points are shown for comparison only.  
 Solid black line is from Neuman (MO0003SZFWTEEP.000).  
 Solid blue line is from Bedinger et al. (1989).  
 Solid pink line is from Gelhar (MO0003SZFWTEEP.000).  
 Solid blue block is effective porosity value from NC-EWDP-19D1 (BSC 2003d, Section 6.5).  
 Solid black triangle is mean matrix porosity (DOE 1997, Table 8-1).  
 Diamond outlined shapes are total porosity (Burbey and Wheatcraft 1986).  
 X is total porosity (DOE 1997, Table 8-2).  
 Square outlined shape is mean bulk porosity (DOE 1997, Table 8-1).

Figure H-1. Effective Porosity Distributions and Point Estimates of Effective and Total Porosity in Alluvium

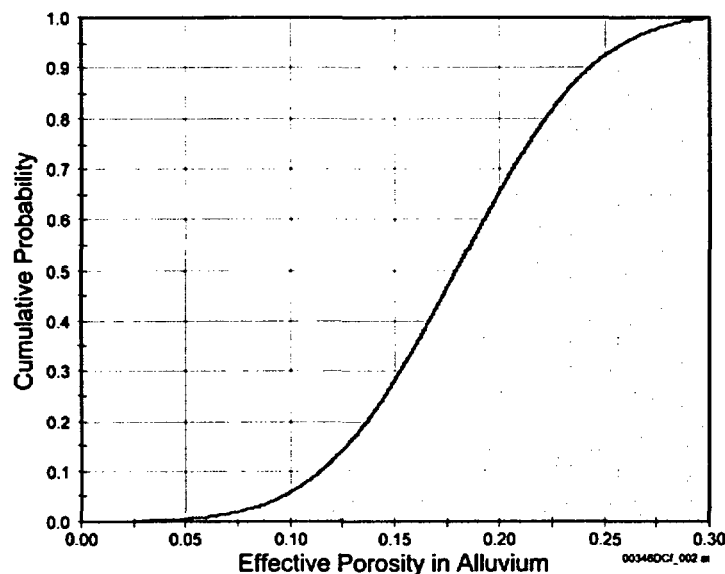
The upper bound of the uncertainty distribution for effective porosity was reevaluated because of new site-specific data obtained since the total system performance assessment for the site recommendation. The new upper bound is based on the total porosity values from borehole NC-EWDP-19D1 and corroborative data. The total porosity values from corroborative sources are shown in Table H-1, which have an average value of 0.35. A borehole gravimetry log of NC-EWDP-19D1 (BSC 2003d) resulted in an average porosity estimate of 0.24 for the saturated alluvium at this location, with a minimum value of 0.18 (local value from one measurement “station”) and a maximum value of 0.29 (DTN: MO0105GPLOG19D.000).

Table H-1. Summary of Corroborative Values of Total Porosity ( $\phi_T$ )

| Reference                               | Total Porosity | Comments  |
|---|----------------|---|
| DOE (1997, Table 8-1)                   | 0.36           | Mean bulk porosity                                    |
| DOE (1997, Table 8-2)                   | 0.35           | Total porosity  |
| Burbey and Wheatcraft (1986, pp. 23-24) | 0.34           | Average of porosity values from Table 3 of that study |
| Average of above                        | 0.35           | N/A   |

Source: BSC 2003e, Table 6-10.

The average of the corroborative values in Table H-1 and the average of the site-specific data from borehole NC-EWDP-19D1 were used to develop the upper bound of the effective porosity uncertainty distribution. The average value of 0.35 (Table H-1) and the average value from NC-EWDP-19D1 of 0.24 yield a mean of 0.30. Figure H-2 shows the truncated normal distribution developed in this analysis for effective porosity in the alluvium with a mean of 0.18, standard deviation of 0.051, a lower bound of 0, and an upper bound of 0.30. The effective porosities for the two alluvium units in the SSFM are sampled independently from this distribution.



Source: BSC 2003e, Figure 6-10.

Figure H-2. Cumulative Distribution Function for Uncertainty in Effective Porosity in the Alluvium

### H.4.3 Flowing Intervals for Tuffs

#### H.4.3.1 Flow Interval Spacing

The flowing interval spacing is a key parameter in the dual porosity model that is included in the saturated zone transport abstraction model (BSC 2003e). A flowing interval is defined as a fractured zone that transmits fluid in the saturated zone, as identified through borehole flow meter surveys (see Figure 3-2 in Section 3.2.1.1 and associated discussion). A detailed description of how uncertainty in the flowing interval spacing is justified is provided in *SZ Flow and Transport Model Abstraction* (BSC 2003e, Section 6.5.2.4).

#### H.4.3.2 Flowing Interval Porosity

The flowing interval porosity is defined as the volume of the pore space through which considerable groundwater flow occurs, relative to the total volume (described in Section 3.2.1). At Yucca Mountain, rather than attempt to define the porosity within all fractures, a flowing interval is defined as the region in which considerable groundwater flow occurs at a borehole. The flowing interval porosity characterizes these flowing intervals rather than all fractures. The advantage to this definition of flowing interval porosity is that in situ borehole data can be used

to characterize the parameter. The flowing interval porosity also may include the matrix porosity of small matrix blocks within fracture zones that potentially experience rapid matrix diffusion. A detailed description of uncertainty in the flowing interval porosity is provided in *SZ Flow and Transport Model Abstraction* (BSC 2003e, Section 6.5.2.5).

#### **H.4.4 Effective Diffusion Coefficient**

Matrix diffusion, as described in Section 3.3.1.3, is a process in which diffusing particles move, via Brownian motion, through both mobile and immobile fluids. A detailed description of uncertainty in the effective diffusion coefficient provided in *SZ Flow and Transport Model Abstraction* (BSC 2003e, Section 6.5.2.6).

#### **H.4.5 Longitudinal and Transverse Dispersion**

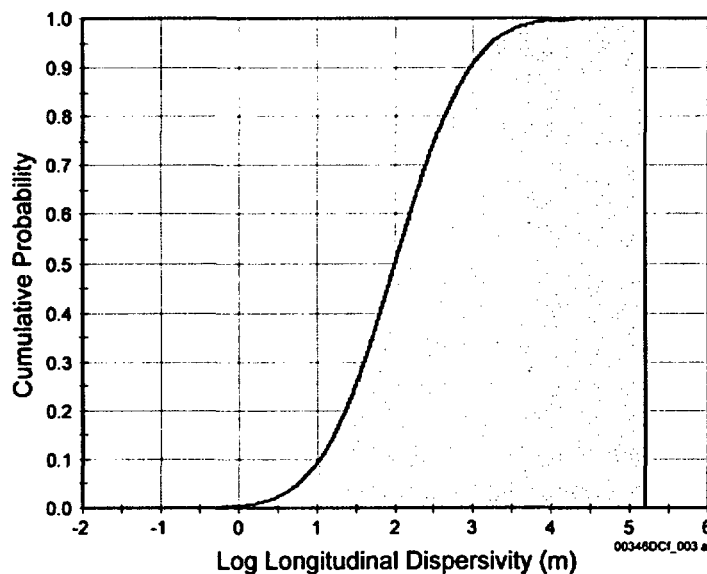
Longitudinal dispersion is the mixing of a solute in groundwater that occurs along the direction of flow (BSC 2003e, Section 6.5.2.9). This mixing is a function of many factors including the relative concentrations of the solute, the velocity pattern within the flow field, and the host rock properties. An important component of dispersion is dispersivity, a coarse measure of the solute (mechanical) spreading properties of the rock. The dispersion process causes spreading of the solute in directions transverse to the flow path and in the longitudinal flow direction (Freeze and Cherry 1979, p. 394). Longitudinal dispersivity is important at the leading edge of the advancing plume, while transverse dispersivity (horizontal transverse and vertical transverse) is the strongest control on plume spreading and dilution (CRWMS M&O 1998, p. LG-12). Because the entire mass of radionuclides potentially released is mixed into the regulatory volume, the plume-spreading effects of transverse dispersion are irrelevant for total system performance assessment calculations.

Temporal changes in the groundwater flow field may increase the apparent dispersivity displayed by a contaminant plume, particularly with regard to transverse dispersion. However, the thick unsaturated zone in the area of Yucca Mountain likely dampens the response of the saturated zone flow system to seasonal or decadal variations in infiltration.

These dispersivities (longitudinal, vertical transverse, and horizontal transverse) are used in the advection-dispersion equation governing solute transport and are implemented in the saturated zone transport abstraction model (BSC 2003e) as stochastic parameters. Recommendations from the expert elicitation were used as the basis for specifying the distribution for longitudinal and transverse dispersivity. As part of the expert elicitation, Dr. Lynn Gelhar provided statistical distributions for longitudinal dispersivity at 5 and 30 km (CRWMS M&O 1998, p. 3-21). These distributions for longitudinal dispersivity are consistent with his previous work (Gelhar 1986, pp. 135s to 145s). The transverse and longitudinal dispersion that may occur at the sub-gridblock scale within the SSFM have been estimated (CRWMS M&O 2000, p. 53). McKenna et al. (2003) also describes the estimation of dispersivity using sub-gridblock scale modeling. The results from this report are in general agreement with the estimates by the expert elicitation panel (CRWMS M&O 2000, p. 55). However, there was a large difference in the 500-m spatial scale at which the analyses were conducted (CRWMS M&O 2000) and the 5- and 30-km scales at which the expert elicitation (CRWMS M&O 1998) estimates were made. Nonetheless, both sources of information are mutually supportive.

In the saturated zone transport abstraction model (BSC 2003e), longitudinal dispersivity is sampled as a log-transformed parameter, and transverse dispersivities are calculated as indicated by the expert elicitation (CRWMS M&O 1998, p. 3-21).

The log-normal distribution for longitudinal dispersivity over the approximately 18 km transport distance in the saturated zone is specified as  $E[\log_{10}(\alpha_L)] = 2.0$  and  $S.D.[\log_{10}(\alpha_L)] = 0.75$ . The cumulative distribution function of uncertainty in longitudinal dispersivity is shown in Figure H-3.



Source: BSC 2003e, Figure 6-10.

Figure H-3. Cumulative Distribution Function for Uncertainty in Longitudinal Dispersivity over the Approximately 18-km Travel Distance in the Saturated Zone

#### H.4.6 Other Transport Parameters

The remaining solute transport parameters show less variability and have a smaller effect on transport predictions. These parameters include matrix porosity (BSC 2003e, Section 6.5.2.18), bulk density of the volcanic matrix (BSC 2003e, Section 6.5.2.19), and bulk density of the alluvium (BSC 2003e, Section 6.5.2.7).

### H.5 REFERENCES

#### H.5.1 Documents Cited

Bedinger, M.S.; Sargent, K.A.; Langer, W.H.; Sherman, F.B.; Reed, J.E.; and Brady, B.T. 1989. Studies of Geology and Hydrology in the Basin and Range Province, Southwestern United States, for Isolation of High-Level Radioactive Waste—Basis of Characterization and Evaluation. U.S. Geological Survey Professional Paper 1370-A. Washington, D.C.: U.S. Government Printing Office. ACC: NNA.19910524.0125.

Broxton, D.E.; Warren, R.G.; Hagan, R.C.; and Luedemann, G. 1986. Chemistry of Diagenetically Altered Tuffs at a Potential Nuclear Waste Repository, Yucca Mountain, Nye County, Nevada. LA-10802-MS. Los Alamos, New Mexico: Los Alamos National Laboratory. ACC: MOL.19980527.0202.

BSC (Bechtel SAIC Company) 2003a. *Saturated Zone Colloid Transport*. ANL-NBS-HS-000031 REV 01A. Las Vegas, Nevada: Bechtel SAIC Company. ACC: MOL.20030602.0288.

BSC 2003b. *Site-Scale Saturated Zone Transport*. MDL-NBS-HS-000010 REV 01A. Las Vegas, Nevada: Bechtel SAIC Company. ACC: MOL.20030626.0180.

BSC 2003c. *Radionuclide Transport Models Under Ambient Conditions*. MDL-NBS-HS-000008 REV 01D. Las Vegas, Nevada: Bechtel SAIC Company. ACC: MOL.20030922.0196.

BSC 2003d. *Saturated Zone In-Situ Testing*. ANL-NBS-HS-000039 REV 00A. Las Vegas, Nevada: Bechtel SAIC Company. ACC: MOL.20030602.0291.

BSC 2003e. *SZ Flow and Transport Model Abstraction*. MDL-NBS-HS-000021 REV 00A. Las Vegas, Nevada: Bechtel SAIC Company. ACC: MOL.20030612.0138.

Burbey, T.J. and Wheatcraft, S.W. 1986. *Tritium and Chlorine-36 Migration from a Nuclear Explosion Cavity*. DOE/NV/10384-09. Reno, Nevada: University of Nevada, Desert Research Institute, Water Resources Center. TIC: 201927.

Codell, R.B.; Byrne, M.R.; McCartin, T.J.; Mohanty, S.; Weldy, J.; Jarzempa, M.; Wittmeyer, G.W.; Lu, Y.; and Rice, R.W. 2001. *System-Level Repository Sensitivity Analyses, Using TPA Version 3.2 Code*. NUREG-1746. Washington, D.C.: U.S. Nuclear Regulatory Commission (NRC). TIC: 254763.

CRWMS M&O (Civilian Radioactive Waste Management System Management and Operating Contractor) 1998. *Saturated Zone Flow and Transport Expert Elicitation Project*. Deliverable SL5X4AM3. Las Vegas, Nevada: CRWMS M&O. ACC: MOL.19980825.0008.

CRWMS M&O 2000. *Modeling Sub Gridblock Scale Dispersion in Three-Dimensional Heterogeneous Fractured Media (S0015)*. ANL-NBS-HS-000022 REV 00 ICN 01. Las Vegas, Nevada: CRWMS M&O. ACC: MOL.20001107.0376.

DOE (U.S. Department of Energy) 1997. *Regional Groundwater Flow and Tritium Transport Modeling and Risk Assessment of the Underground Test Area, Nevada Test Site, Nevada*. DOE/NV-477. Las Vegas, Nevada: U.S. Department of Energy. ACC: MOL.20010731.0303.

Freeze, R.A. and Cherry, J.A. 1979. *Groundwater*. Englewood Cliffs, New Jersey: Prentice-Hall. TIC: 217571.

Gelhar, L.W. 1986. "Stochastic Subsurface Hydrology from Theory to Applications." *Water Resources Research*, 22, (9), 135S-145S. Washington, D.C.: American Geophysical Union. TIC: 240749.

Kotra, J.P.; Lee, M.P.; Eisenberg, N.A.; and DeWispelare, A.R. 1996. *Branch Technical Position on the Use of Expert Elicitation in the High-Level Radioactive Waste Program*. NUREG-1563. Washington, D.C.: U.S. Nuclear Regulatory Commission. TIC: 226832.

McKenna, S.A.; Walker, D.D.; and Arnold, B. 2003. "Modeling Dispersion in Three-Dimensional Heterogeneous Fractured Media at Yucca Mountain." *Journal of Contaminant Hydrology*, 62-63, 577-594. New York, New York: Elsevier. TIC: 254205.

NRC (U.S. Nuclear Regulatory Commission) 1999. *NRC Sensitivity and Uncertainty Analyses for a Proposed HLW Repository at Yucca Mountain, Nevada, Using TPA 3.1, Results and Conclusions*. NUREG-1668. Volume 2. Washington, D.C.: U.S. Nuclear Regulatory Commission. TIC: 248805.

Reamer, C.W. and Gil, A.V. 2001. Summary Highlights of NRC/DOE Technical Exchange and Management Meeting of Range of Thermal Operating Temperatures, September 18-19, 2001. Washington, D.C.: U.S. Nuclear Regulatory Commission. ACC: MOL.20020107.0162.

Reamer, C.W. and Williams, D.R. 2000. Summary Highlights of NRC/DOE Technical Exchange and Management Meeting on Radionuclide Transport. Meeting held December 5-7, 2000, Berkeley, California. Washington, D.C.: U.S. Nuclear Regulatory Commission. ACC: MOL.20010117.0063.

Schlueter, J. 2002. "Radionuclide Transport Agreement 2.03 and 2.04." Letter from J. Schlueter (NRC) to J.D. Ziegler (DOE/YMSCO), August 30, 2002, 0909024110, with enclosure. ACC: MOL.20020916.0098.

Ziegler, J.D. 2002. "Transmittal of Reports Addressing Key Technical Issues (KTI)." Letter from J.D. Ziegler (DOE/YMSCO) to J.R. Schlueter (NRC), April 30, 2002, 0501022470, OL&RC:TCG-1045, with enclosures. ACC: MOL.20020730.0636.

## **H.5.2 Data, Listed by Data Tracking Number**

LA0302AM831341.002. Unsaturated Zone Distribution Coefficients (KDS) for U, NP, PU, AM, PA, CS, SR, RA, and TH. Submittal date: 02/04/2003.

MO0003SZFWTEEP.000. Data Resulting from the Saturated Zone Flow and Transport Expert Elicitation Project. Submittal date: 03/06/2000.

MO0105GPLOG19D.000. Geophysical Log Data from Borehole NC EWDP 19D. Submittal date: 05/31/2001.

**APPENDIX I**  
**TRANSPORT—SPATIAL VARIABILITY OF PARAMETERS**  
**(RESPONSE TO RT 2.02, TSPAI 3.32, AND TSPAI 4.02)**

### **Note Regarding the Status of Supporting Technical Information**

This document was prepared using the most current information available at the time of its development. This Technical Basis Document and its appendices providing Key Technical Issue Agreement responses that were prepared using preliminary or draft information reflect the status of the Yucca Mountain Project's scientific and design bases at the time of submittal. In some cases this involved the use of draft Analysis and Model Reports (AMRs) and other draft references whose contents may change with time. Information that evolves through subsequent revisions of the AMRs and other references will be reflected in the License Application (LA) as the approved analyses of record at the time of LA submittal. Consequently, the Project will not routinely update either this Technical Basis Document or its Key Technical Issue Agreement appendices to reflect changes in the supporting references prior to submittal of the LA.

## APPENDIX I

### TRANSPORT—SPATIAL VARIABILITY OF PARAMETERS (RESPONSE TO RT 2.02, TSPA 3.32, AND TSPA 4.02)

This appendix provides a response for Key Technical Issue (KTI) agreements Radionuclide Transport (RT) 2.02, Total System Performance Assessment and Integration (TSPA) 3.32 and TSPA 4.02. These agreements relate to providing more information about the treatment of spatial variability and uncertainty in transport parameters.

#### I.1 KEY TECHNICAL ISSUE AGREEMENTS

##### I.1.1 RT 2.02, TSPA 3.32, and TSPA 4.02

KTI agreement RT 2.02 was reached during the U.S. Nuclear Regulatory Commission (NRC)/U.S. Department of Energy (DOE) technical exchange and management meeting on radionuclide transport held December 5 through 7, 2000, in Berkeley, California. Radionuclide transport KTI subissues 1, 2, and 3 were discussed at that meeting (Reamer and Williams 2000).

KTI agreements TSPA 3.32 and TSPA 4.02 were reached during the NRC/DOE technical exchange and management meeting on total system performance assessment and integration held August 6 through 10, 2001, in Las Vegas, Nevada. TSPA KTI subissues 1, 2, 3, and 4 were discussed at that meeting (Reamer 2001).

Wording of the agreements is as follows:

##### RT 2.02

The DOE should demonstrate that TSPA captures the spatial variability of parameters affecting radionuclide transport in alluvium. DOE will demonstrate that TSPA captures the variability of parameters affecting radionuclide transport in alluvium. This information will be provided in the TSPA-LA document due in FY 2003.

##### TSPA 3.32<sup>1</sup>

Provide the technical basis that the representation of uncertainty in the saturated zone as essentially all lack-of-knowledge uncertainty (as opposed to real sample variability) does not result in an underestimation of risk when propagated to the performance assessment (SZ2.4.1).

DOE will provide the technical basis that the representation of uncertainty (i.e., lack-of-knowledge uncertainty) in the saturated zone does not result in an underestimation of risk when propagated to the performance assessment. A deterministic case from Saturated Zone Flow Patterns and Analyses AMR (ANL-NBS-HS-000038) will be compared to TSPA analyses. The comparison

---

<sup>1</sup> SZ2.4.1 in this agreement refers to NRC integrated subissue SZ 2 (NRC 2002, Table 1.1-2).

will be documented in the TSPA for any potential license application expected to be available to NRC in FY 2003.

#### **TSPA I 4.02**

DOE will provide the documentation that supports the representation of distribution coefficients ( $K_d$ s) in the performance assessment as uncorrelated is consistent with the physical processes and does not result in an underestimation of risk. This will be documented in the TSPA for any potential license application in FY2003.

#### **I.1.2 Related Key Technical Issue Agreements**

TSPA I 3.32, related to the spatial variability of saturated zone transport properties, is closely related to TSPA I 3.31, which deals with temporal variability of saturated zone transport properties. The response to TSPA I 3.31 is presented in Appendix L, where it is concluded that temporal variability in sorption characteristics is affected only by temporal changes in water chemistry that are captured in the distributions of  $K_d$  (Appendix L, Section L.4).

### **I.2 RELEVANCE TO REPOSITORY PERFORMANCE**

The purpose of the site-scale saturated zone flow and transport model is to describe the spatial and temporal distribution of groundwater as it moves from the water table below the potential repository, through the saturated zone, and to the point of uptake by the receptor of interest. The saturated zone processes that control the movement of groundwater and the movement of dissolved radionuclides and colloidal particles that might be present, and the processes that reduce radionuclide concentrations in the saturated zone, are affected by spatial variability of the saturated zone materials.

The geologic media encountered at Yucca Mountain are inherently heterogeneous. This heterogeneity is reflected in spatial variabilities in the geologic media's physical and chemical properties. The degree of spatial correlation between these spatially heterogeneous characteristics and the parameters used to describe these spatially heterogeneous properties is uncertain. Yucca Mountain Project model development for the saturated zone flow and transport model considered the effects variability in the development and propagation of uncertainties from experimental data into the abstraction process. The abstraction of radionuclide transport in the saturated zone for total system performance assessment analyses is developed using a site-scale, three-dimensional, single-continuum, particle-tracking transport model. Particle transport pathways are calculated based on spatially variable groundwater flux vectors (flow fields) derived from the site-scale saturated zone flow model (SSFm). It is necessary to provide experimental and field information to constrain data uncertainty for transport parameters relevant to the saturated zone system performance.

This technical basis document describes spatial variability in the context of the saturated zone conceptual understanding relevant to assessing the flow of groundwater and transport of radionuclides in the saturated zone beneath and downgradient from Yucca Mountain. This uncertainty manifests itself in the uncertainty in the advective-dispersive transport times of radionuclides important to postclosure performance assessment presented in Section 3.4.

### I.3 RESPONSE

**Response to RT 2.02**—Geologic systems are inherently heterogeneous, reflected in considerable spatial variability in physical and chemical properties. It would be ideal if all of such variability were incorporated in numerical modeling of subsurface flow and transport. However, such an approach quickly becomes impractical for most real-world problems due to data and computational limitations. In order to best account for the effects of spatial variability in a model that already accounts for numerous complex processes, the Performance Assessment model uses the Monte Carlo approach in conjunction with parameter distributions of effective parameters to predict flow and transport at Yucca Mountain.

Parameter uncertainties are quantified using uncertainty distributions, which numerically represent the state of knowledge about a particular parameter on the scale of the model domain. The uncertainty distribution of a parameter (either cumulative distribution function or probability density function), represents what is known about the parameter, and it reflects the current understanding of the range and likelihood of the appropriate parameter values when used in these models (BSC 2002, p. 45). The uncertainty distributions incorporate uncertainties associated with field or laboratory data, knowledge of how the parameter will be used in the model, and theoretical considerations. The subgrid-scale spatial variability is implicitly considered in these parameter value distributions. Correlation lengths for a particular parameter must be smaller than the model domain in order to use these effective parameters. In order to use the effective parameters that have been developed, large correlated structures the size of the model domain must not exist. The very limited data that exist to evaluate correlation length in alluvium are consistent in that their correlation lengths are less than the model domain. Small correlation lengths result in a simulation sampling the entire distribution making it possible to represent the small-scale heterogeneity with an effective parameter. In other words, there is no “connected pathway” of high effective porosity or low effective sorption coefficient in the alluvium that could invalidate the use of effective parameters in the total system performance assessment model. Finally, it is assumed that correlations between various parameters in the model do not need to be considered. Painter et al. (2001) examined the correlation between hydraulic conductivity and distribution coefficient and did not find the correlation to be important.

In summary, due to the large transport distances of interest and the small correlation lengths, the effects of spatial variability mitigated due to averaging that occurs at the large scales of interest. Section 4 provides the technical justification for these positions for the cases of flow, transport, and sorption.

**Response to TSPAI 3.32**—Uncertainty exists in a number of the parameters that affect groundwater flow and radionuclide transport through the saturated zone. These parameters include the fraction of the groundwater travel path that is in the alluvial aquifer, the groundwater flux along this travel path, the spacing between the fracture intervals into which this flux is distributed within the tuff aquifers, the effective porosity within the flowing intervals of the fractured tuff and the porous alluvial materials, the matrix diffusion coefficient representative of the fractured tuff, and the radionuclide sorption coefficient ( $K_d$ ). Uncertainty in these parameters has been explicitly included in the abstraction of advective-dispersive transport velocities and in the resulting transport time between the point where radionuclides enter the saturated zone and the compliance boundary.

Uncertainty in the saturated zone flow and transport model results in a range of projected advective-dispersive transport times for each radionuclide, which can be represented by a series of mass (or activity) breakthrough curves. Mass breakthrough curves illustrate the range of possible outcomes for a given release of radionuclides from the unsaturated zone to the saturated zone and then through the saturated zone to the compliance boundary. Due to uncertainty in a number of important parameters, a relatively wide range of advective-dispersive transport times is possible. Most of the projected transport times for unretarded radionuclides such as iodine, technetium and carbon fall within the range of a few hundred to a few thousand years, which is consistent with the range of transport times based on the interpretation of  $^{14}\text{C}$  groundwater ages in the saturated zone (see Section 3.2.3). It is important to note that an individual breakthrough curve is not, in itself, the result of uncertainty. Even if the system were understood perfectly, radionuclides would travel at different speeds and produce a distribution of transport times.

For unretarded species such as technetium, the results indicate that about 5 percent of the realizations have median breakthrough times of less than about 1,000 years, while about 6 percent have median breakthrough times of greater than 10,000 years. Short transport times generally are attributed to short travel paths in the alluvium, high groundwater fluxes, large spacing between flowing intervals, and low effective porosity in the fractured tuff aquifers. Long transport times generally are attributed to long travel paths in the alluvium, low groundwater fluxes, and high effective porosities in the alluvium. Each breakthrough curve is equally likely, and each represents a possible result of the behavior of the saturated zone.

The uncertainty in transport velocities and transport times is directly propagated to the estimation of risk using the total system performance assessment model. Although this model will be fully described in the total system performance assessment for the license application model and analysis document, the basic tenets of this approach can be described with a simple example. Suppose an activity flux of 1 pCi/yr of technetium occurs at the base of the unsaturated zone starting at 3,000 years. Although there is uncertainty in the magnitude, location, and timing of this release, for this example, assume that the flux in each realization occurs at the same magnitude, at the same place and starts at the same time. Based on saturated zone transport uncertainty, there is some possibility that this activity flux would be transported to the point of compliance in a few hundred years, resulting in an activity flux into the annual water demand of the reasonably maximally exposed individual of 1 pCi/yr. Most of the transport times are between several hundred and several thousand years, so most of the realizations would result in a mass breakthrough within the 10,000-year regulatory period. However, there is a small possibility (on the order of 10 percent of the realizations have median advective-dispersive

transport times of greater than 7,000 years) that the technetium transport would be sufficiently delayed to not arrive at the compliance point within the 10,000-year compliance period. In this example, about 90 percent of the time the complete breakthrough of the activity flux would occur during the compliance period, with 10 percent of the realizations having no activity flux within the compliance period. Thus, the mean activity flux (in pCi/yr) at the compliance point (which would be directly translated into the mean dose) would be 90 percent of the incoming activity flux at the base of the unsaturated zone. This is not an underestimation of risk; it is the effect of the uncertainty in the advective-dispersive transport velocity propagated through a valid computational approach.

To further illustrate this effect, a comparison was made between the multiple advective-dispersive transport realizations abstracted into the system performance model to capture parameter uncertainty and a single realization using the mean of the input values for the parameters described above. The results of the mean-value realization may be considered representative of the model abstraction if there were no uncertainty (i.e., every realization would have a relative mass breakthrough equal to the mean breakthrough curve). Examining the neptunium breakthrough results for the mean-value case at 10,000 years, about 5 percent of the mass released from the unsaturated zone at time zero would be calculated to be released at the compliance point. This contrasts with the observation from the multiple uncertainty realizations that about 30 percent of the realizations would have released 50 percent of the mass. Note that the median transport times represent the time that 50 percent of a unit release to the saturated zone is released at the compliance boundary. This implies that when averaged over all realizations, the mean activity flux at the compliance point would be about 15 percent of the initial activity flux, a factor of 3 times greater than the single deterministic realization using the mean-value of the inputs without considering the effects of uncertainty. This comparison indicates that the risk is not underestimated when the uncertainty in the transport times is considered in the analysis.

In summary, these analyses indicate that the uncertainty representation in the saturated zone flow and transport model is appropriate and does not underestimate the risk when propagated to the total system performance assessment.

**Response to TSPAI 4.02**—In contrast to the saturated zone transport model used in the abstraction of saturated zone transport in the site recommendation analyses, correlation between sorption coefficients has been considered in the license application saturated zone transport model. Correlation factors have been derived for the sampling of sorption coefficient probability density functions for neptunium, plutonium, and uranium transported in the saturated zone (BSC 2003a, Attachment I). The sorption coefficient for neptunium and uranium is considered to be correlated with a correlation of 0.75 between the tuff and alluvial aquifers. Neptunium and uranium are considered to be correlated with a coefficient of 0.5. The nonsorbing radionuclides such as carbon, technetium, and iodine are all considered to have no sorption. Similarly, the highly sorbed radionuclides such as americium, protactinium, and thorium are considered to have similar sorption coefficient distributions.

The information in this report is responsive to agreements RT 2.02, TSPAI 3.32, and TSPAI 4.02 made between the DOE and NRC. The report contains the information that the DOE considers necessary for the NRC to review for closure of these agreements.

## **I.4 BASIS FOR THE RESPONSE**

### **I.4.1 Spatial Variability (Response to RT 2.02)**

#### **I.4.1.1 Background on Spatial Variability**

The principal parameters for which sub-grid block spatial variability are of concern for performance predictions are permeability, effective porosity, and sorption coefficients. Analysis of the impact of spatial variability of flow and transport parameters (e.g., permeability and effective porosity) is studied by estimating the uncertainty in parameter values from available experimental data and incorporating these uncertainty estimates in the total system performance assessment calculations. The impact of a spatially variable sorption coefficient on travel time in the fractured volcanic tuffs is evaluated in detail using a geostatistical approach. Distributions of effective  $K_d$  for uranium, neptunium, cesium, and plutonium (used in total system performance assessment calculations) were calculated by determining effective retardation resulting from a spatially heterogeneous  $K_d$  field. These spatially heterogeneous  $K_d$  fields were calculated using geostatistical methods.

Geologic formations are inherently heterogeneous, reflecting considerable spatial variability in physical and chemical properties. It would be ideal if all such variabilities were incorporated in numerical modeling. However, such an approach becomes impractical for most real-world problems because an overwhelmingly large number of nodes would be needed for a numerical model to precisely represent spatial variability. Recently, research has been devoted to effectively and efficiently incorporate the impacts of geologic variability in subsurface flow and transport (Zhang 2002).

Formation material properties, including fundamental parameters such as permeability and porosity, are ordinarily observed at only a few locations despite the fact that they exhibit a high degree of spatial variability at all length scales. This combination of considerable spatial heterogeneity with a relatively small number of observations leads to uncertainty about the values of the formation properties, and thus, to uncertainty in estimating or predicting flow in such formations. The theory of stochastic processes provides a natural method for evaluating uncertainties. In stochastic formalism, uncertainty is represented by probability (or by related quantities such as statistical moments). Because material parameters such as permeability and porosity are not purely random, they are treated as random space functions with variabilities exhibiting some spatial correlation structures. The spatial correlations may be quantified by joint (multi-variable, multi-point, or both) probability distributions or joint statistical moments such as cross- and auto-covariances. In turn, equations governing subsurface flow and transport become stochastic differential equations, the solutions of which are no longer deterministic, but probability distributions of flow and transport quantities. Generally, stochastic differential equations cannot be solved exactly, but estimates of the first few moments of the corresponding probability distribution can be made (namely the mean, variance, and covariances). These moments are sufficient to approximate the confidence intervals.

Moment equation and Monte Carlo simulation are two commonly used methods for solving (approximating) stochastic differential equations. In moment equation methods, equations governing the statistical moments of flow quantities are first derived from the (original)

stochastic differential equations, which are then solved numerically or analytically. This method directly yields the statistical moments. Monte Carlo simulation is an alternative, and perhaps the most straightforward method, for solving stochastic equations. This widely used approach is conceptually simple and is based on the idea of approximating stochastic processes using a large number of equally probable realizations.

The moment equation and Monte Carlo simulation methods have been used to derive effective parameters of flow and transport, including hydraulic conductivity, porosity, dispersivity, and retardation coefficients (Zhang 2002). The effective parameters are commonly used for describing the mean behaviors of the systems or subsystems under study (see Appendix H, Section H-3). However, not only the mean behaviors, but also uncertainties about them, are needed for better describing flow and transport in the subsurface.

The total system performance assessment model uses the Monte Carlo approach in conjunction with parameter distributions of effective parameters to predict flow and transport at Yucca Mountain. Parameter uncertainties are quantified using uncertainty distributions, which numerically represent the state of knowledge about a particular parameter on the scale of the model domain. The uncertainty distribution of a parameter (either cumulative distribution function or probability density function) represents what is known about the parameter, and it reflects the current understanding of the range and likelihood of the appropriate parameter values when used in these models (BSC 2002, p. 45). The uncertainty distributions incorporate uncertainties associated with field or laboratory data, knowledge of how the parameter will be used in the model, and theoretical considerations. The subgrid-scale spatial variability is implicitly considered in the parameter value distributions. The Monte Carlo approach, which samples from these parameter distributions, includes the effects of spatially variable parameters on overall system uncertainty. The following sections provide the technical justification for this position for the cases of flow, transport, and sorption.

#### **I.4.1.2 Spatial Variability in Flow and Transport Parameters**

The principal parameters for which subgrid-block spatial variability are of concern for performance predictions are permeability, effective porosity, and sorption coefficients. Analysis of the impact of spatial variability of flow and transport parameters (e.g., permeability and effective porosity) is treated in this section, whereas the spatial variability of sorption coefficients is treated in detail in the next section.

It is important to recognize the role of permeability and porosity in flow and transport model predictions. Transport times through the alluvium are governed by the water flux, the effective porosity through which radionuclides travel, and sorption coefficients. Average permeabilities are estimated by calibrating the saturated zone flow model to potentiometric and water flux data. Because the model assumes homogeneity within a hydrostratigraphic unit, this approach inherently provides an estimate of the mean permeability of the unit (i.e., the effective permeability at the scale of a hydrogeologic unit). Uncertainty in the effective permeability is addressed by considering a range of flux values (BSC 2003b).

In addition to groundwater flux, the effective porosity used in large-scale flow and transport simulations could also be influenced by heterogeneity in the medium. The approach to

considering these effects is through the use of an “effective porosity” approach that considers the possibility of nonuniform transport through the alluvium. Consider a system in which the groundwater flux through a portion of the medium is obtained from flow model calibration assuming homogenous, intra-unit properties. If the medium is highly heterogeneous at smaller scales, water and radionuclides will likely travel through only a portion of the available pore space. A method for capturing this effect in large-scale simulations is by applying a lower porosity for the medium than would be obtained from examination of cores. Under steady state flow conditions, a lower porosity would have no impact on groundwater flow simulations, but would decrease transport times, all else being equal. Estimates of the total porosity of the alluvial material fall in the range of 0.12 to 0.36 (Bedinger et al. 1989, p. A18, Table 1; Burbey and Wheatcraft 1986, pp. 23 and 24; DOE 1997). However, the effective porosity used in total system performance assessment modeling has a mean of 0.18 and a range from 0.02 to 0.3 (BSC 2003b). For the sake of example, assume 0.3 for total porosity as a means for discussing the issue, the mean value implies transport through  $0.18/0.3 = 0.6$  or 60 percent of the entire medium. In contrast, the lower limit of 0.02 yields transport through  $0.02/0.3 = 0.067$  or 6.7 percent of the medium, and the upper limit on effective porosity is essentially homogeneous transport ( $0.3/0.3 = 1$ ). In essence, the model accounts for preferential flow and transport caused by heterogeneous properties through a reduction of the effective porosity. By using values as low as 6.7 percent of the total available porosity, even though the unit is porous and permeable, the influence of heterogeneities in alluvium porosity has been conservatively bounded.

#### **I.4.1.3 Spatial Variability of the Distribution Coefficient**

In this section, the impact of small-scale variability in the distribution coefficient on travel times is studied. The basic conclusion from this sorption analysis for applicability to transport in the alluvium is that the correlation lengths for a particular parameter must be smaller than the model domain in order to use these effective parameters. In order to use the effective parameters that have been developed, large correlated structures the size of the model domain must not exist. The very limited data that exist to evaluate correlation length in alluvium are consistent in that their correlation lengths are less than the model domain. Small correlation lengths result in a simulation sampling the entire distribution making it possible to represent correlation length of the distribution coefficient as much smaller than the model domain. Specifically, that there are no large connected pathways of permeability or distribution coefficient in the alluvium. A transporting radionuclide will sample the entire range of distribution coefficients, and a transported particle that samples the entire distribution can be represented by an effective distribution coefficient.

Radionuclide transport is affected by natural spatial variability in hydrologic and chemical properties. Proper assessment of the impact of these variabilities on radionuclide transport is important when determining the long-term fate of radionuclides and associated exposure risks. Effects of small-scale variability on groundwater flow and transport have been studied using stochastic techniques (Gelhar 1993; Zhang 2002). This appendix outlines the derivations of distributions of effective sorption coefficients for multiple radionuclides. These distributions are used to simulate transport of radionuclides in the saturated zone site-scale model during total system performance assessment calculations. In total system performance assessment calculations, radionuclide transport is modeled using a single value of  $K_d$  for grid blocks with dimensions  $500 \times 500$  m in the  $x$  and  $y$  directions. It is assumed that the uniform single value

captures the processes that affect transport through the grid block. In the field, values of  $K_d$  are variable at scales smaller than 500 m. Thus, if a uniform single value of  $K_d$  is used to model sorption, it is important to use a value that effectively captures variability at smaller scale and results in the same sorption behavior as if the small-scale processes were represented explicitly. The factors that affect the sorption behavior of the rock matrix include mineral composition, ground water chemistry, and the type of radionuclide. Mineral composition and groundwater chemistry are spatially variable at a scale smaller than 500 m. This spatial variability should be taken into account when modeling sorption behavior. In addition, if laboratory measurements are used to model sorption at scales much larger than the scale of laboratory measurements, it is important to consider the effect of scale. It should be noted that the stochastic nature of the flow model will effectively account for small-scale heterogeneities through use of a wide range of  $K_d$ s for the single model grid blocks.

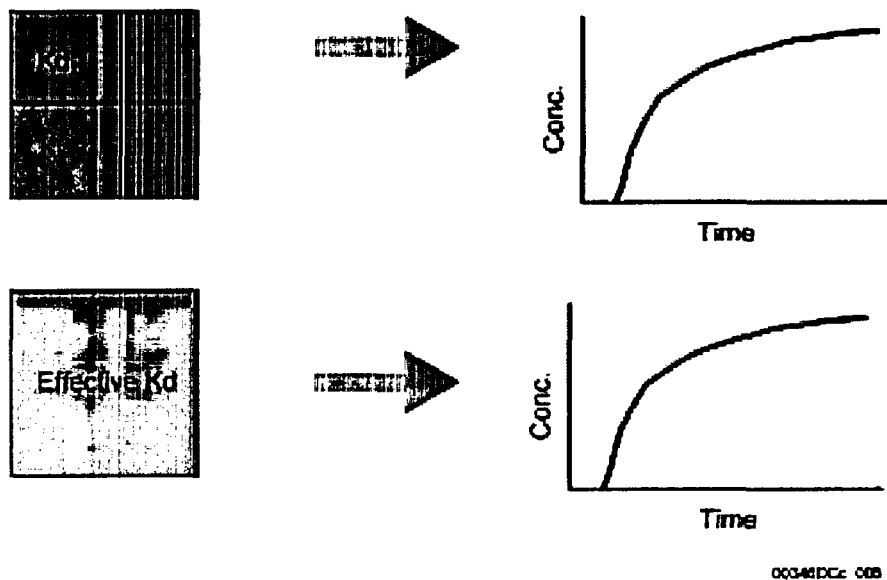
This section summarizes the approach used to calculate effective values of  $K_d$  for a  $500 \times 500 \times 100$  m grid block while incorporating the effect of small-scale spatial heterogeneity in  $K_d$  values, the effect of upscaling, and the effect of mineralogy. The approach includes generating spatially heterogeneous distributions of  $K_d$  at a scale much smaller than 500 m using the heterogeneous distributions to calculate effective  $K_d$  values. The heterogeneous distributions were generated by incorporating the effect of spatial variability in rock mineralogy. A stochastic approach was used to generate distributions of effective  $K_d$  values, and multiple  $K_d$  realizations were used to calculate effective  $K_d$  values. The input data used to generate the heterogeneous  $K_d$  distributions were derived from experimental data described in *Site-Scale Saturated Zone Transport* (BSC 2003a, Attachment I).

#### I.4.1.3.1 Approach

**Definition of Effective  $K_d$** —Effective  $K_d$  is defined as the value of  $K_d$  that would result in a radionuclide sorption behavior that is similar to the sorption behavior resulting from a heterogeneous distribution of small-scale  $K_d$  values as illustrated in Figure I-1, in which a two-dimensional grid block with a uniform effective  $K_d$  produces radionuclide breakthrough behavior that is similar to that shown by the same grid block with four subgrid blocks with different  $K_d$  properties.

With the above definition, the following approach was used to compute an effective  $K_d$ . The retardation coefficient and  $K_d$  are related to each other as

$$K_d = (\text{retardation coefficient} - 1) \frac{\text{Porosity}}{\text{Bulk Density}} \quad (\text{Eq. I-1})$$



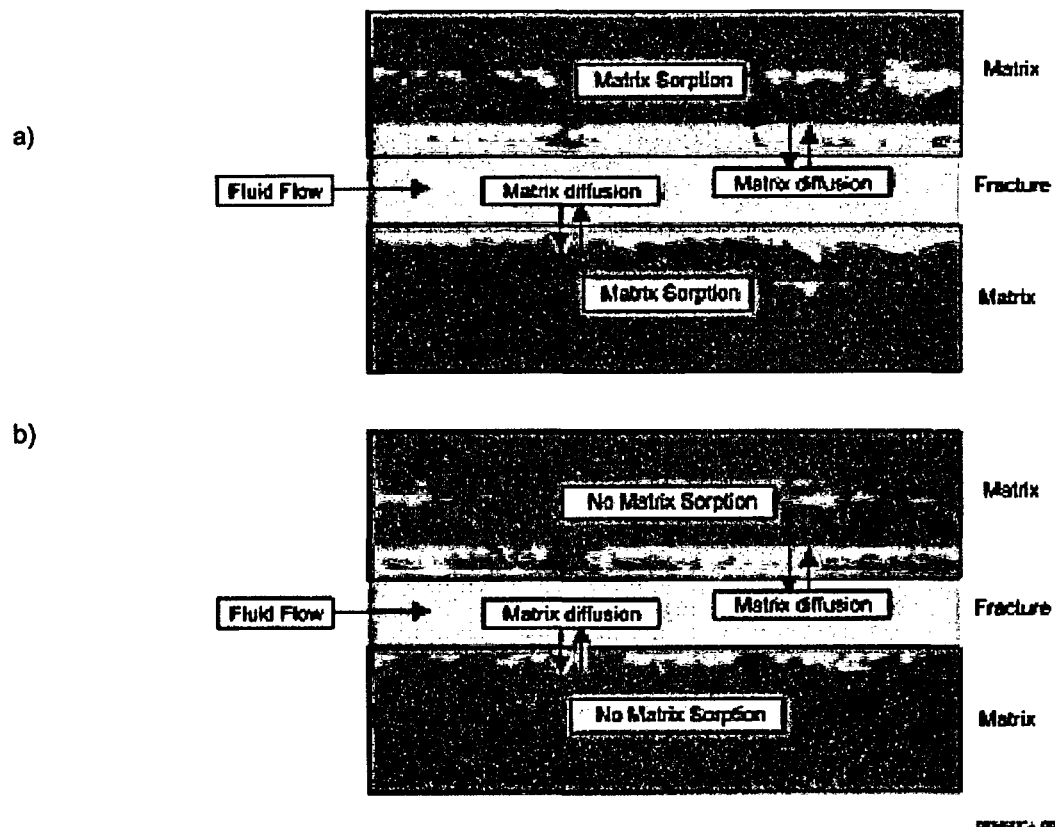
Source: BSC 2003a, Figure III-1

Figure I-1. A Schematic Representation of the Definition of Effective  $K_d$

Thus, if the retardation behavior of a system is well characterized, it can be used to calculate the effective  $K_d$ . Effective retardation behavior of a grid block for a particular radionuclide was determined by comparing two breakthrough curves for the same grid block under identical flow conditions. A breakthrough curve was calculated assuming dual-porosity transport in which the radionuclide can diffuse from fracture to matrix subject to retardation (Figure I-2a). A second curve was calculated with identical diffusion behavior but assuming no retardation in matrix (Figure I-2b). In both calculations, retardation on fracture surfaces was neglected. Using these two curves, effective matrix retardation was calculated by comparing the breakthrough times for 50 percent relative concentration. These breakthrough curves are illustrated, with and without matrix sorption, in Figure I-3.

The breakthrough curve for the case with no matrix sorption is much steeper than that for the case with matrix sorption. The times at which 50 percent breakthrough takes place are marked as  $T_1$  and  $T_2$  for the cases without matrix sorption and with matrix sorption, respectively. The effective retardation coefficient was calculated as the ratio of these two times:

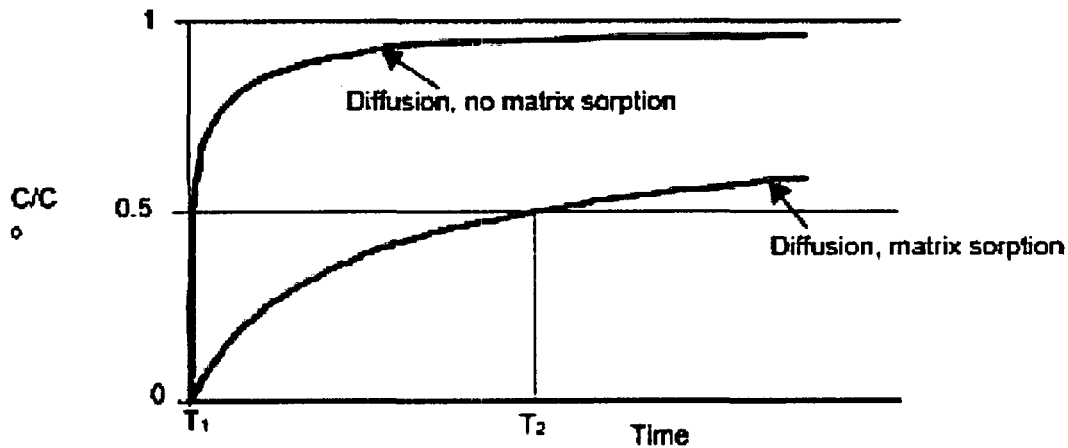
$$\text{Effective Retardation } (R_{\text{eff}}) = \frac{T_2}{T_1} \quad (\text{Eq. I-2})$$



Source: BSC 2003a, Figure III-2

NOTE: Diagram at top shows transport with diffusion followed by matrix sorption.  
Diagram at bottom shows transport with diffusion followed by no matrix sorption.

Figure I-2. The Processes During Transport of a Radionuclide in Fractured Media



00348DCe\_007

Source: BSC 2003a, Figure III-3

Figure I-3. Representation of the Breakthrough Curves Used to Calculate Effective Matrix Retardation Behavior

This definition of effective retardation was used to calculate effective  $K_d$  values using Equation I-1. Multiple values of effective  $K_d$  were calculated using multiple spatially heterogeneous realizations of  $K_d$  and subsequently were used to generate a statistical distribution of effective  $K_d$ . The heterogeneous  $K_d$  distributions were generated geostatistically. Before describing the approach, a brief discussion on the method used to perform transport calculations follows.

**Transport Calculations**—A dual-porosity transport model was used to calculate the breakthrough curves. The calculations were performed using the streamline particle-tracking macro “*sptr*” in the Finite Element Heat and Mass Transport Code (LANL 2003). The dual-porosity transport model in the “*sptr*” macro is based on the analytical solution developed by Sudicky and Frind (1982) for radionuclide transport in a system of parallel fractures. This solution takes into account advective transport in the fractures, molecular diffusion from the fracture into the porous matrix, and adsorption on the fracture surface as well as within the matrix. In this model all of the above mentioned processes except adsorption on the fracture surface are represented. It is conservatively assumed that there is no sorption on the fracture surfaces.

**Stochastic Realizations of  $K_d$** —The value of  $K_d$  depends on several factors, including rock mineralogy and water chemistry, as well as spatial location. This dependence was taken into account when developing  $K_d$  realizations. Groundwater chemistry was treated as a spatially random variable, and its effect on  $K_d$  values was incorporated in the  $K_d$  distribution used as input for generating stochastic realizations (BSC 2003a). Dependence on rock mineralogy was captured with spatial realizations of rock mineralogy. Data on mineral abundance in rock were available from X-ray diffraction analysis of samples from multiple wells. These mineral abundance data were used to determine prevalent mineralogic rock types. Spatial correlation functions were calculated from these data and were subsequently used to generate multiple realizations of spatial distribution of rock types using sequential indicator simulations.

Sequential indicator simulation is a powerful tool that can be used to generate stochastic realizations of parameters. It uses cumulative distribution functions of observed data as input and estimates a discrete, nonparametric true cumulative distribution function of a simulated parameter. An indicator is a variable used to indicate the presence or absence of any parameter qualitatively or quantitatively. For example, an indicator can be used to define the presence of a particular rock type at any spatial location. It can also be used to define whether the value of a parameter falls within a certain range of parameter values defined as cutoffs.

After the spatial distributions of rock types were generated, experimental data on  $K_d$  values were used to generate spatial distributions of  $K_d$  values. The experimental data were analyzed to derive rock-type specific statistical distributions for  $K_d$ . The statistical distributions were used to derive the cumulative distribution function for each radionuclide. Next, indicators were defined at four cumulative distribution function cutoffs of 0.2, 0.4, 0.6, and 0.8. These cutoffs, along with the spatial correlation information, were used to generate spatial distributions. Unlike mineral abundance data, spatial information on  $K_d$  observations was not available. As a result, no spatial correlation functions were available for  $K_d$  data. Four different values were used for correlation length in the horizontal direction to investigate its effects on spatial  $K_d$  distributions:

- Correlation length equal to a single grid block dimension (4 m) that represents spatially random realizations;
- Correlation length equal to the correlation length used to generate permeability realizations (60 m);
- Correlation length equal to the large grid block length (500 m); and
- Correlation length equal to the correlation length used to generate rock-type data.

The above values represent the expected range of correlation lengths for  $K_d$ . The  $K_d$  correlation length in the vertical direction, as well as the correlation lengths for rock types and permeability, were not varied. The spatial distributions of  $K_d$  realizations were also generated using the sequential indicator simulation approach. These spatial distributions of  $K_d$  values were generated for individual rock types. Distributions for each rock type were generated independent of other rock-type distributions. Finally, the rock-type specific  $K_d$  distributions and rock-type distributions were used to generate integrated  $K_d$  distributions. The approach used is explained schematically below:

$$\begin{aligned}
 &K_d \text{ distribution for rock-type '1': } K_{d1}^1, K_{d2}^1, K_{d3}^1, K_{d4}^1, K_{d5}^1, K_{d6}^1, K_{d7}^1, \dots, K_{dn}^1 \\
 &K_d \text{ distribution for rock-type '0': } K_{d1}^0, K_{d2}^0, K_{d3}^0, K_{d4}^0, K_{d5}^0, K_{d6}^0, K_{d7}^0, \dots, K_{dn}^0 \\
 &\text{Rock-type distribution: } 1, 0, 1, 1, 1, 0, 0, \dots, 1 \\
 &\text{Combined } K_d \text{ distribution: } K_{d1}^1, K_{d2}^0, K_{d3}^1, K_{d4}^1, K_{d5}^1, K_{d6}^0, K_{d7}^1, \dots, K_{dn}^1
 \end{aligned}$$

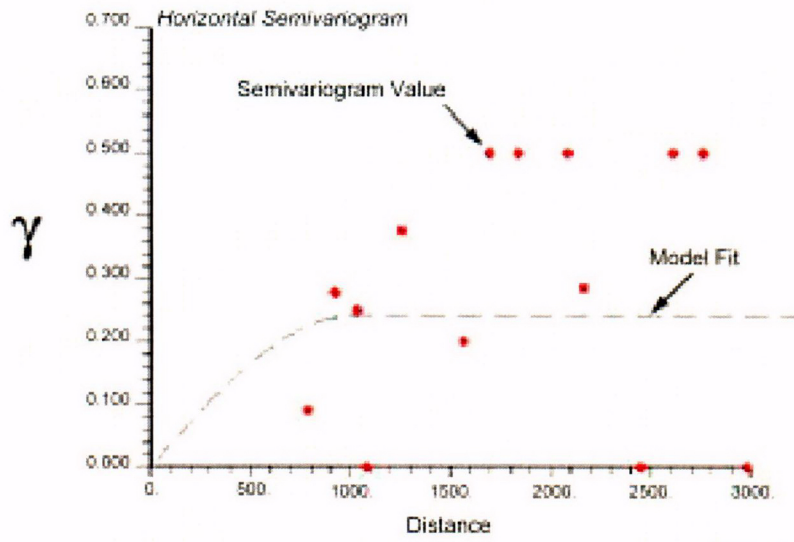
The approach explained above incorporates the effect of spatial heterogeneity and rock mineralogy on the spatial distribution of  $K_d$ . Multiple realizations for the spatial distribution of  $K_d$  values were generated with this approach.

**Stochastic Realizations of Permeability**—Similar to the  $K_d$  distributions, spatial distributions of permeability were generated using the stochastic approach. The approach and data used were similar to that found in *Modeling Sub Gridblock Scale Dispersion in Three-Dimensional Heterogeneous Fractured Media (S0015)* (CRWMS M&O 2000). These permeability realizations represent and encompass continuum distributions of permeability for fractured rocks. In this analysis, permeability and  $K_d$  were treated as independent, uncorrelated parameters.

#### **I.4.1.3.2 Results**

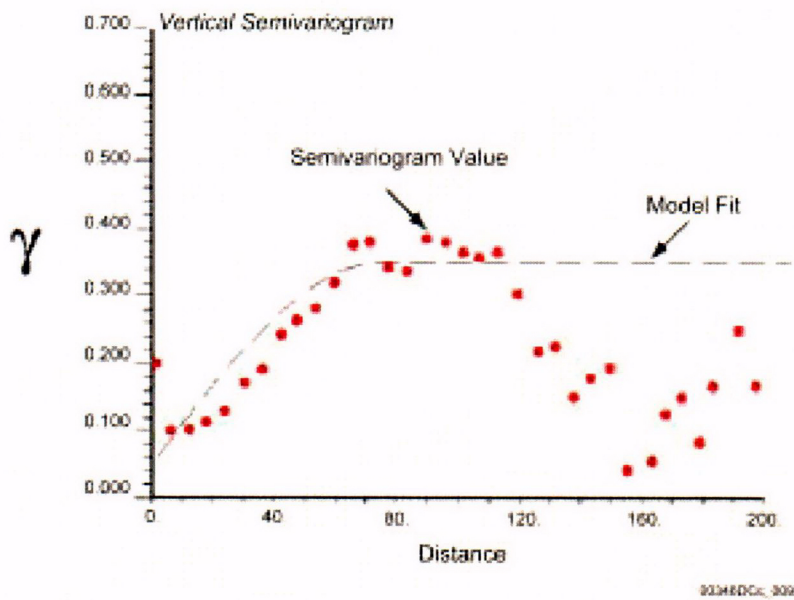
**Stochastic Realizations of  $K_d$** —As mentioned in *Site-Scale Saturated Zone Transport* (BSC 2003a, Section III.2.3), the first step in generating realizations for the spatial distribution of  $K_d$  values was to generate a mineralogic rock-type realization. Mineral abundance data for rock samples from multiple wells were used. The mineral abundance data include the following minerals: smectites, zeolites, tridymite, cristobalite, quartz, feldspar, volcanic glass, analcime, mica, and calcite. These data were used to identify rock types using the following definition: the rock type was labeled as zeolitic if the zeolitic abundance was greater than 20 percent, as vitric if glass abundance was greater than 80 percent, and as devitrified otherwise.

Only the data that were part of the saturated zone extending 200 m below the water table were used in this analysis. When mineralogic abundance data were converted to rock-type data with the above definition, it was observed that only zeolitic and devitrified rocks were present for the top 200 m of the saturated zone. The observed proportions of the rocks were 60 percent zeolitic and 40 percent devitrified. The data set also included information on the spatial location of rock samples. These data were used to calculate spatial correlation information through indicator semivariograms. Two directional semivariograms were calculated: one in the horizontal direction and another in the vertical direction. The semivariograms were used to calculate the correlation information. The semivariograms and the correlation functions fit to them are shown in Figures I-4 and I-5. For the horizontal semivariogram the sill is assumed to be the variance of the input data due to lack of sufficient pairs at higher separations. The parameters for the model fit are shown in Table I-1. The semivariogram adequately fits the data.



Source: BSC 2003a, Figure III-4

Figure I-4. Calculated Semivariogram and Model Fit in the Horizontal Direction



Source: BSC 2003a, Figure III-5

Figure I-5. Calculated Semivariogram and Model Fit in the Vertical Direction

Table I-1. Spatial Correlation Parameters for Mineralogic Rock Type Data

| Direction  | Range (m) | Sill |
|------------|-----------|------|
| Horizontal | 1000      | 0.25 |
| Vertical   | 75        | 0.35 |

Source: BSC 2003a, Table III-2.

These correlation parameters were used to generate spatial distributions of rock types. The sequential indicator simulation algorithm SISIM, which is part of GSLIB, was used to generate these distributions. Five different rock-type realizations were generated using this approach. The proportions of zeolitic and devitrified rocks in the five output realizations were in good agreement with the input proportions.

Spatial realizations for  $K_d$  were generated for four different radionuclides: uranium, neptunium, cesium, and plutonium. The statistical distributions of the experimentally available data for these radionuclides are given in Table I-2.

Table I-2. Statistical Distributions of Experimentally Observed  $K_d$  Values

| Radionuclide | Rock-type   | Distribution | Mean    | Standard Deviation | Minimum | Maximum |
|--------------|-------------|--------------|---------|--------------------|---------|---------|
| Uranium      | zeolitic    | Normal       | 12.0    | 3.6                | 5.0     | 20.0    |
|              | devitrified | Normal       | 2.0     | 0.6                | 0.0     | 4.0     |
| Cesium       | zeolitic    | Exponential  | 16942.0 | 14930.0            | 2000.0  | 42000.0 |
|              | devitrified | Normal       | 728.0   | 464.0              | 100.0   | 1000.0  |
| Neptunium    | zeolitic    | Normal       | 2.88    | 1.47               | 0.0     | 6.0     |
|              | devitrified | Exponential  | 0.69    | 0.707              | 0.0     | 2.0     |
| Plutonium    | zeolitic    | Beta         | 100.0   | 15.0               | 50.0    | 300.0   |
|              | devitrified | Beta         | 100.0   | 15.0               | 50.0    | 300.0   |

Source: BSC 2003a, Table III-4.

These distributions were used to derive the cumulative distribution functions for each radionuclide for each rock type. For each cumulative distribution function, indicators were defined at four cumulative distribution function cutoffs: 0.2, 0.4, 0.6, and 0.8. In the absence of spatial data, correlation lengths were parameterized, and four different correlation lengths were used to generate stochastic realizations. This effect of correlation length was studied only for uranium. For other radionuclides, a correlation length of 500 m was used. Fifty different realizations were generated for each radionuclide and each rock type. Statistics of the output realizations were calculated and found to be in very good agreement with the input data statistics. These rock-type specific  $K_d$  distributions were combined to generate distributions that were conditioned to the realizations of rock types.

**Results of Breakthrough Curve Calculations Using the Particle-Tracking Algorithm**—These multiple  $K_d$  realizations were used to compute breakthrough curves and model the sorption behavior of each radionuclide. A two-step approach was used. In the first step, steady-state flow fields were computed for fifty different permeability realizations. The properties used for these

calculations are shown in Table I-3. Note that the parameters such as matrix porosity, fracture porosity, and fracture density were not treated as stochastic variables in this analysis.

Table I-3. Values of Properties Used in Flow and Transport Calculations

| Property                               | Value                |
|--|----------------------|
| Matrix Porosity                        | 0.22                 |
| Rock Bulk Density (kg/m <sup>3</sup> ) | 1997.5               |
| Fracture Porosity                      | 0.001                |
| Fracture Spacing (m)                   | 19.49                |
| Hydraulic Gradient (m/m)               | $2.9 \times 10^{-4}$ |

Source: BSC 2003c, Table III-9.

The above values were obtained from experimental measurements taken at the Yucca Mountain site. Values for fracture spacing and aperture are the mean of available measurements. Values for matrix porosity and rock bulk density are averages for the following units: Topopah Spring, Calico Hills, Prow Pass, Bullfrog, and Tram. These are the main units observed in the saturated zone 200 m below the water table.

Steady-state flow fields were used in the particle-tracking calculations. The flow fields were calculated using constant head at two ends and no flux boundary conditions on the sides, top, and bottom. As mentioned earlier, the particle-tracking macro "sptr" of Finite Element Heat and Mass Transport Code (LANL 2003) was used to model transport. In these calculations, 4,000 particles were released along one face of a 500-m model element and were allowed to move under the influence of the steady-state flow field. The locations of the particle releases were determined by a flux-weighted placement scheme. Two sets of particle-tracking calculations were performed for each steady-state flow field. In the first set of calculations, the baseline breakthrough curve was calculated assuming transport with diffusion from fracture to matrix without matrix sorption. In the second set of calculations, the breakthrough curve was calculated assuming transport with diffusion followed by sorption on the matrix. For these calculations, the stochastically generated  $K_d$  distributions were used. The values of the diffusion coefficient used for these calculations are shown in Table I-4. The diffusion coefficient was not treated as a stochastic variable and the values fall in the range of the effective diffusion coefficient used for total system performance assessment calculations.

Table I-4. Values of Diffusion Coefficients Used for the Particle-Tracking Calculations

| Radionuclide                 | Diffusion Coefficient (m <sup>2</sup> /s) |
|------------------------------|---|
| Uranium                      | $3.2 \times 10^{-11}$                     |
| Plutonium, Cesium, Neptunium | $1.6 \times 10^{-10}$                     |

Source: BSC 2003a, Table III-10.

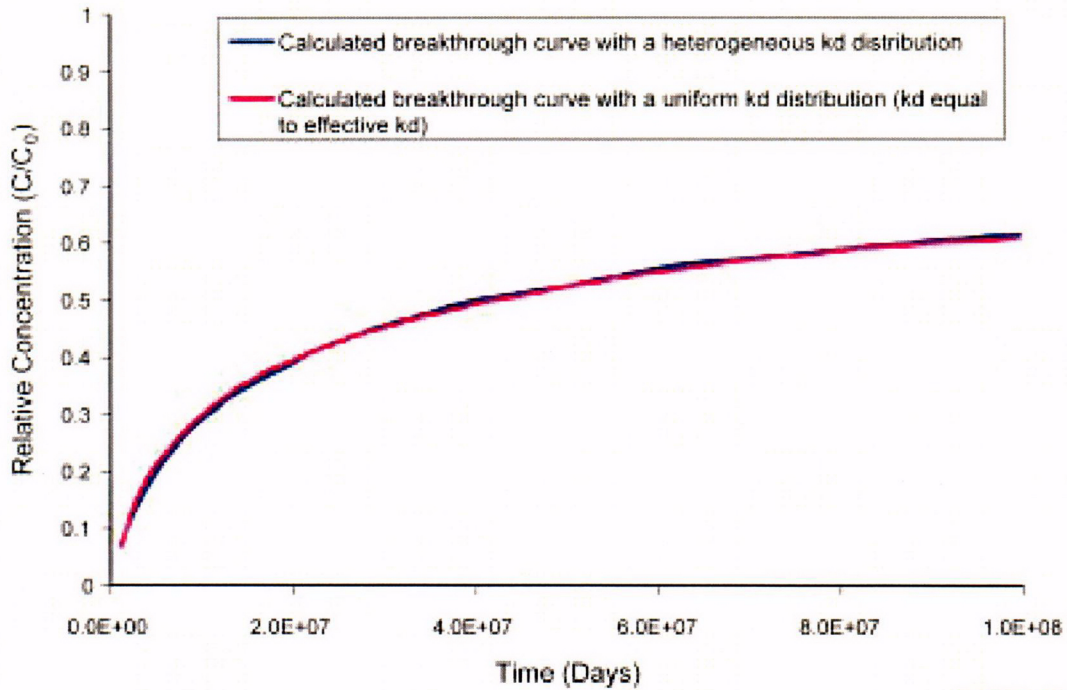
Breakthrough curves subject to effective  $K_d$  values were generated for 50 realizations of  $K_d$ . The statistics of the calculated effective  $K_d$  values are provided in Table I-5. These calculations of stochastic realizations of  $K_d$  were performed using a correlation length of 500 m. As indicated in Table I-5, the effective  $K_d$  distributions are very narrow compared to the distributions of experimentally observed  $K_d$  values (see Table I-2).

Table I-5. Statistics of Calculated Effective  $K_d$  Values

| Radionuclide | Mean    | Standard Deviation | Minimum | Maximum |
|--------------|---------|--------------------|---------|---------|
| Uranium      | 6.61    | 0.61               | 5.39    | 8.16    |
| Cesium       | 5188.72 | 941.55             | 3000.59 | 6782.92 |
| Plutonium    | 110.17  | 7.45               | 89.90   | 129.87  |
| Neptunium    | 1.48    | 0.23               | 0.99    | 1.83    |

Source: BSC 2003a, Table III-11.

A comparison was made as to how well the calculated effective  $K_d$  values predicted the particle breakthrough behavior with respect to the breakthrough behavior predicted by the heterogeneous  $K_d$  field (from which the effective value was calculated). In these calculations, a uniform value of  $K_d$  equal to the effective  $K_d$  value was used. Figure I-6 shows the two breakthrough curves for one of the  $K_d$  realizations. The effective value of  $K_d$  calculated for this realization was 7.32. As can be seen from the figure, the calculated effective  $K_d$  value captures the breakthrough behavior of the heterogeneous  $K_d$  field well.



0034603c\_010

Source: BSC 2003a, Figure III-16.

Figure I-6. Comparison of Breakthrough Behavior Predicted by the Calculated Effective  $K_d$

**Effect of Horizontal Correlation Length on Effective  $K_d$  Distributions of Uranium**—The effect of correlation length in the horizontal direction on effective  $K_d$  values was investigated. In these calculations the correlation length in the vertical direction was not varied. The correlation length for permeability is provided by *Modeling Sub Gridblock Scale Dispersion in Three-Dimensional Heterogeneous Fractured Media* (CRWMS M&O 2000). In these calculations, permeability and  $K_d$  are assumed to be uncorrelated. Table I-6 details the statistics

of the calculated effective  $K_d$  values along with the correlation length used to generate the heterogeneous  $K_d$  distributions. As can be seen from the results, variation in the correlation length does not greatly affect the calculated statistics of effective  $K_d$  values.

Table I-6. Effect of Changes in Correlation Length on Effective  $K_d$  Distributions

| Correlation Length (m) | Mean | Standard Deviation | Minimum | Maximum |
|------------------------|------|--------------------|---------|---------|
| 4                      | 6.71 | 0.49               | 5.70    | 8.13    |
| 60                     | 6.79 | 0.47               | 5.42    | 8.14    |
| 500                    | 6.61 | 0.61               | 5.39    | 8.16    |
| 1000                   | 6.58 | 0.62               | 4.46    | 7.85    |

Source: BSC 2003a, Table III-16.

**Effect of Variability in the Hydraulic Gradient**—The effect of variability in the hydraulic gradient on calculated effective  $K_d$  values was studied. These calculations were performed only for uranium and used  $K_d$  realizations generated with a correlation length of 500 m. Two different values of hydraulic gradient were used:  $8.7 \times 10^{-4}$  m/m (3 times mean hydraulic gradient) and  $0.967 \times 10^{-4}$  m/m (one-third of mean hydraulic gradient). Steady-state flow fields were calculated with these hydraulic gradients and were subsequently used to calculate particle breakthrough curves. The statistics of the resulting effective  $K_d$  values are compared to those calculated using a mean hydraulic gradient of  $2.9 \times 10^{-4}$  m/m in Table I-7. Variability of an order of magnitude in hydraulic gradient has little effect on the effective  $K_d$  distributions.

Table I-7. Statistics of Calculated Effective  $K_d$  Values for Different Hydraulic Gradients

| Hydraulic Gradient     | Mean | Standard Deviation | Minimum | Maximum |
|------------------------|------|--------------------|---------|---------|
| $0.967 \times 10^{-4}$ | 6.55 | 0.59               | 5.13    | 7.53    |
| $2.9 \times 10^{-4}$   | 6.61 | 0.61               | 5.39    | 8.16    |
| $8.7 \times 10^{-4}$   | 6.27 | 0.56               | 4.97    | 7.65    |

Source: BSC 2003c, Table III-13.

#### I.4.1.3.3 Summary

Studies were performed to calculate distributions of effective  $K_d$  for uranium, neptunium, cesium, and plutonium. These effective  $K_d$  distributions are used in the total system performance assessment calculations. The effective  $K_d$  distributions were calculated through a stochastic approach in which multiple values of effective  $K_d$  were calculated. The value of effective  $K_d$  was determined by calculating effective retardation resulting from a spatially heterogeneous  $K_d$  field. The spatially heterogeneous  $K_d$  fields were calculated using geostatistics. The factors affecting the spatial distribution of  $K_d$ , such as rock mineralogy and spatial heterogeneity, were taken into account while generating the heterogeneous  $K_d$  fields. The correlation lengths used to generate the fields were parameterized. The conclusions of the study are that:

- The calculated effective  $K_d$  values closely reproduced the sorption behavior of the heterogeneous  $K_d$  field, validating the approach used to determine the effective  $K_d$  values;

- The distributions of calculated effective  $K_d$  fields were much narrower than the distributions used as the input. This is to be expected because, in any upscaling study, as the scale gets larger the variability in parameter values gets smaller;
- Variability in correlation length had little effect on the effective  $K_d$  distributions for uranium; and
- Variability in hydraulic gradient did not greatly change the effective  $K_d$  distributions.

Once again, it must be reiterated that these small-scale studies of heterogeneity should be viewed in the context of the entire site-scale model. Even though results of the present analysis indicate that variability at a correlation length of 1,000 m is not significantly different than that at 500 m, it should be noted that there may be an upper limit to the correlation length that will yield a single effective  $K_d$  value. However, so long as the correlation lengths are smaller than the scale of transport, effective  $K_d$  values appear to be tightly clustered around a weighted average of the mean  $K_d$ s for the different rock types present in the control volume and it is appropriate to use a single effective parameter for the control volume. The implication is that over 18 km of transport distance, the effective  $K_d$  value for a given radionuclide should approximate the weighted average of the mean  $K_d$  value for the various rock types encountered along the flow pathway. Furthermore, uncertainty is inherently taken into account in the model through Monte Carlo selections from the distributions of parameters (which inherently include the effects of small scale heterogeneity) for each model realization. Thus, the practice of choosing single  $K_d$  values from distributions for each rock type throughout the entire saturated zone domain for a given total system performance assessment realization should result in greater variability in dose predictions over multiple realizations than if spatial variability in  $K_d$  values were represented in each realization. The basic conclusion from this sorption analysis for applicability to transport in the alluvium is that the correlation length of the distribution coefficient is much smaller than the model domain, thus a transported particle that samples the entire distribution can be represented by an effective distribution coefficient.

#### **I.4.2 Representation of Uncertainty (Response to TSPAI 3.32)**

Uncertainty exists in the expected advective-dispersive radionuclide transport times through the saturated zone to the point of compliance. This uncertainty is the result of uncertainty in the flow and transport properties along the paths of likely radionuclide migration, as well as variability in the parameters used to quantify these properties along the flow paths and the variability in the flow paths themselves. The following paragraphs summarize the sources of uncertainty and variability in the saturated zone flow and transport model abstraction that are relevant to the generation and use of the output of these abstractions in the total system performance assessment. The focus of this discussion is on the uncertainty of transport parameters; the potential temporal variability of transport parameters is primarily a function of changes in chemistry, which are addressed in the response to TSPAI 3.31 (Appendix L).

As presented in Section 2.3.7, uncertainty in the flow path orientation is principally a function of the uncertainty in the SSFM and uncertainty in the permeability anisotropy. These uncertainties result in a range of possible travel-path lengths in the fractured tuff and alluvial aquifers. Variability in the flow rate along the possible flow paths has been considered in the SSFM as has

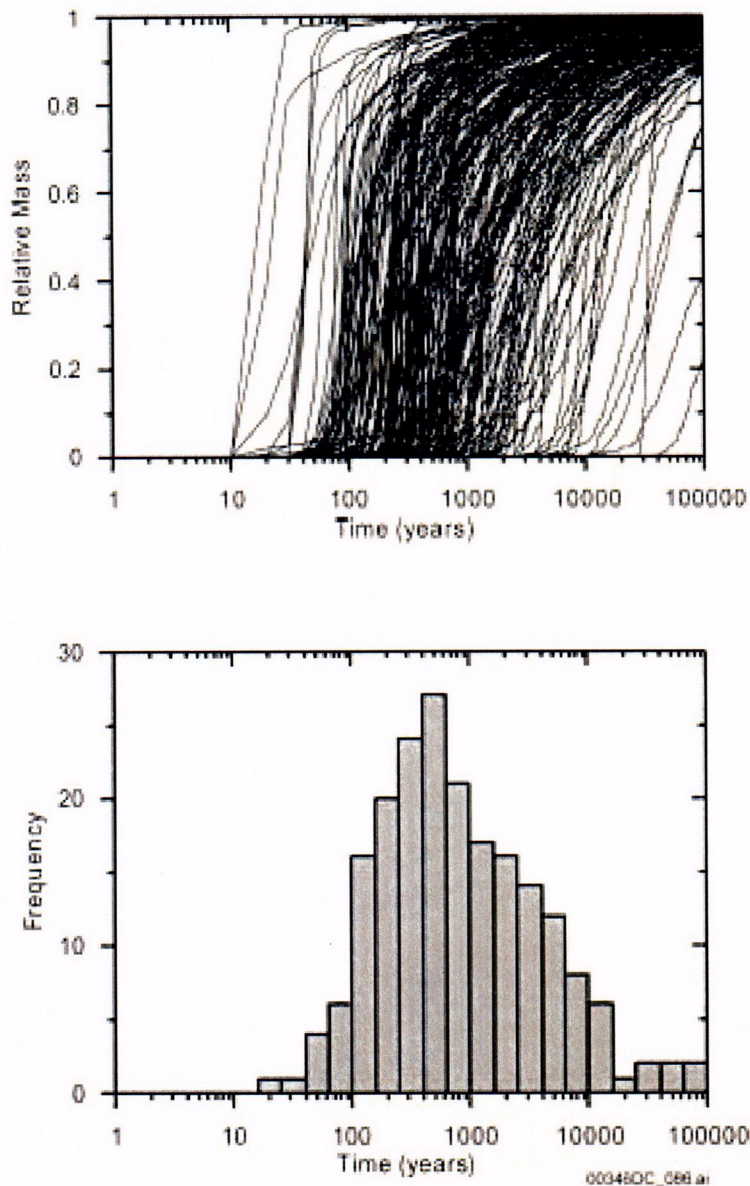
the uncertainty in these flow rates. The uncertainty in the advective flow rates captures the uncertainty in boundary fluxes as well as the uncertainty in the hydraulic properties used in the calibration of the SSFM. In addition to uncertainty and variability in the flow directions and rates, uncertainty in the distribution of the flow within the flowing intervals (as reflected in the flowing interval spacing) is also included in the uncertainty in advective transport times. The flowing interval spacing principally affects the magnitude of the effect of matrix diffusion within the fractured tuff aquifers.

Uncertainty in the transport characteristics of the tuff and alluvial aquifers has been considered in the generation of the range of likely radionuclide delay times within the saturated zone. For example, uncertainty in the matrix diffusion coefficient, effective porosity, and longitudinal dispersivity has been included in the saturated zone flow and transport abstraction model. These uncertainties capture the range of likely conditions that are expected. Although these may be considered a function of space, incorporating the full range of expected conditions from realization to realization assures that the complete uncertainty in expected radionuclide breakthrough is captured in the abstraction. Uncertainty in radionuclide retardation characteristics is directly included in the transport abstraction. This uncertainty captures the scaling of sorption characteristics due to differences in retardation between zeolitic and devitrified tuffs, and it extends the range to cover the possibility that flow is more limited to one or the other of these rock types. In addition, the uncertainty in the transport characteristics of the alluvium, most notably the effective porosity and the sorption coefficients, has been directly included in the model abstraction.

The above uncertainties and variabilities are directly included in the saturated zone flow and transport model abstraction that has been propagated to the total system performance assessment. This uncertainty is represented by a suite of breakthrough curves. Two example breakthrough curves are illustrated in Figures I-7 and I-8 for a nonretarding radionuclide (technetium) and a moderately sorbing radionuclide (neptunium), respectively. These figures illustrate that for nonsorbing radionuclides, about 90 percent of the realizations have median transport times of between 100 and 10,000 years. These distributions, as well as similar distributions for other radionuclides, are directly used in the postclosure performance assessment. They reflect uncertainty in the contribution of the saturated zone in delaying the arrival of radionuclides at the compliance boundary.

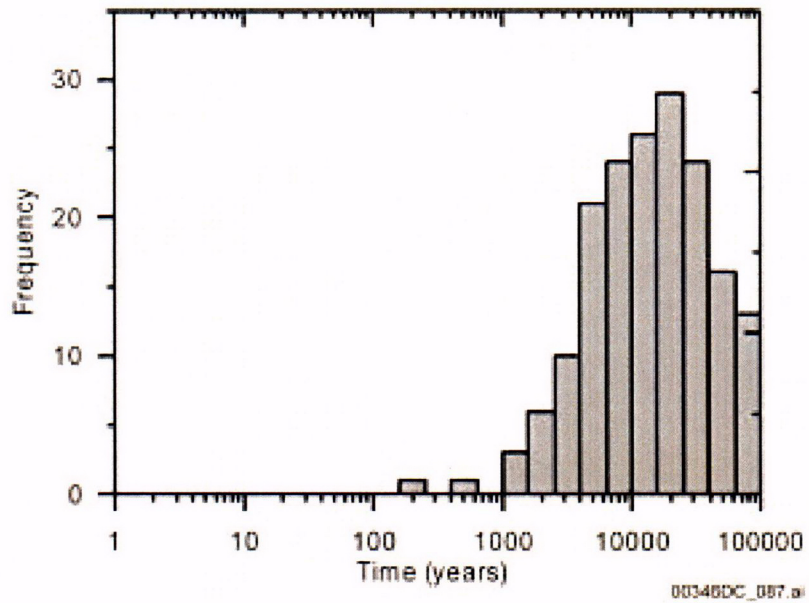
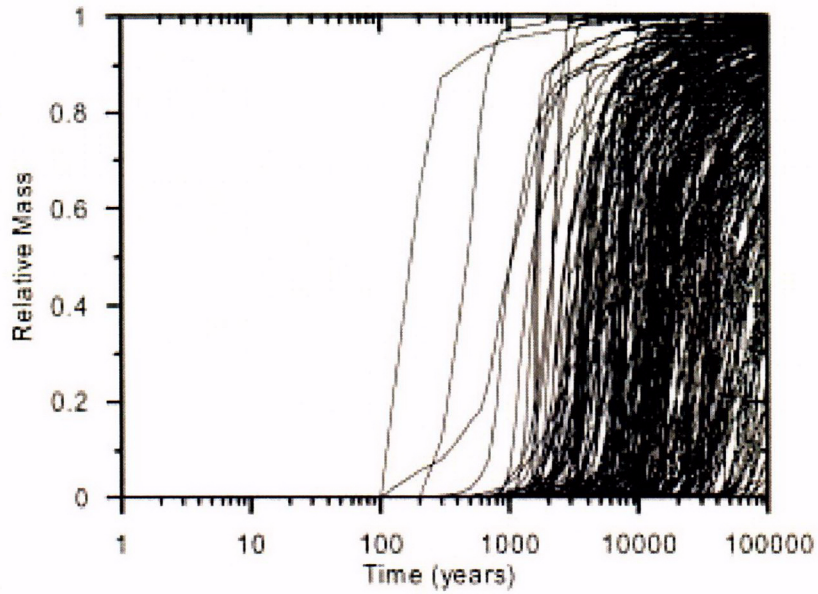
One means of estimating the effect of the uncertainty in these results when they are propagated to the determination of risk in the performance assessment is to compare the full uncertainty distribution to a deterministic realization using the means of the input parameters. The results of a deterministic analysis is presented in Figure I-9. This figure illustrates a single breakthrough curve for technetium and neptunium (as well as two intermediate results for neptunium to separately illustrate the effects of sorption in the fractured tuffs and alluvium). The median breakthrough time for the mean-value realization (about 600 years for technetium and 30,000 years for neptunium as illustrated in Figure I-9) is similar to and slightly greater than the mode of the distribution of median breakthrough times derived from the full distribution of realizations (about 500 years for technetium and about 20,000 years for neptunium as illustrated in Figures I-7 and I-8, respectively).

Examining the neptunium breakthrough curve for the mean-value realization presented in Figure I-9, it can be seen that there is essentially no neptunium released at the compliance boundary until approximately 6,000 years after it has been released into the saturated zone. This compares with the multiple realization results presented in Figure I-8 that indicate about 21 percent of the realizations (42 out of 200) have median neptunium transport times of less than 6,000 years.



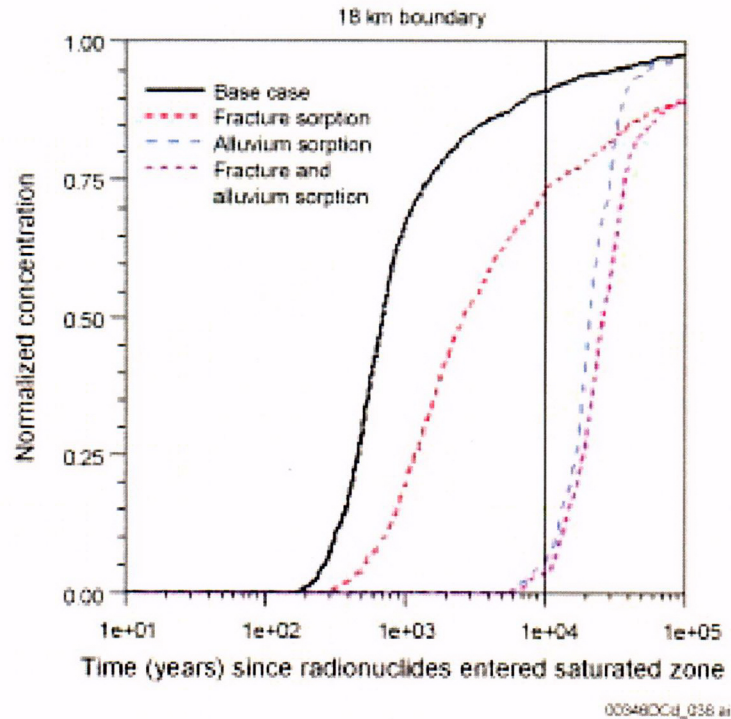
Source: BSC 2003b, Figure 6-28.

Figure I-7. Mass Breakthrough Curves (Upper) and Median Transport Times (Lower) for Carbon, Technetium, and Iodine at 18-km Distance



Source: BSC 2003b, Figure 6-32.

Figure I-8. Mass Breakthrough Curves (Upper) and Median Transport Times (Lower) for Neptunium at 18-km Distance



Source: BSC 2003c, Figure 6.7-1a.

NOTE: Transport trajectories start in the saturated zone beneath the repository and migrate to the compliance point about 18-km south of the repository.

Figure I-9. Predicted Breakthrough Curves

Similarly, the mean value realization results presented in Figure I-9 indicate that at 10,000 years about 5 percent of the neptunium mass released from the unsaturated zone (assuming it had been released to the saturated zone at time zero) would be released into the annual water demand of the reasonably maximally exposed individual. This contrasts with the observation from the multiple uncertainty realizations presented in Figure I-8 that about 30 percent of the realizations (67 realizations out of 200) would have released 50 percent of the mass. Note that the median transport times represent the time that 50 percent of a unit release to the saturated zone is released at the compliance boundary. This implies that when averaged over all realizations, the mean activity flux at the compliance point would be about 15 percent of the initial activity flux, a factor of 3 greater than the single mean value realization without considering the effects of uncertainty.

The above analyses describe the appropriateness of the uncertainty propagation included in the abstraction of advective-dispersive transport times in the saturated zone. In addition, as suggested in the KTI agreement, comparisons have been made with a single value deterministic realization that is analogous to treating all the uncertainty as spatial variability to illustrate that the risk is not being underestimated.

### **I.4.3 Correlations of $K_d$ Distributions (Response to TSPAI 4.02)**

Correlations for sampling sorption-coefficient probability distributions have been derived for the elements americium, neptunium, protactinium, plutonium, thorium, and uranium. The elements americium, protactinium, and thorium sorb primarily by surface-complexation mechanisms and generally have a high affinity for silicate surfaces. As a result, the same sorption-coefficient probability distribution ( $K_d = 1,000\text{--}10,000$  mL/g) has been chosen for all three of these elements. Thus, they are 100 percent correlated. The elements carbon, iodine, and technetium are also 100 percent correlated in that the sorption coefficient is always zero for all three of these elements.

Separate sorption-coefficient probability distributions were derived for neptunium in volcanics and alluvium (BSC 2003a, Section I.8). Controls on the sorption behavior of neptunium are likely to be similar in the volcanic tuffs and the alluvium, due to the similarity in the solution chemistries along the likely flow paths and the significant affect that solution chemistry has on the sorption characteristics. As the detailed mineralogy differences between the tuff and alluvium may affect the sorption behavior, a 75 percent correlation has been chosen for sampling of the neptunium sorption coefficients in volcanics and alluvium. The same arguments apply to uranium. Thus, a 75 percent correlation has also been chosen for sampling of the uranium sorption coefficients in volcanics and alluvium.

The controls on the sorption behavior of neptunium and uranium are similar due to the significant effect that alkalinity has on the sorption characteristics of these radionuclides. To account for these similarities, a correlation of 50 percent was chosen for sampling sorption-coefficient distributions for neptunium and uranium. The above correlations reasonably account for similarities in sorption characteristics of the most significant moderately sorbing radionuclides, neptunium and uranium.

### **I.5 REFERENCES**

Bedinger, M.S.; Sargent, K.A.; Langer, W.H.; Sherman, F.B.; Reed, J.E.; and Brady, B.T. 1989. *Studies of Geology and Hydrology in the Basin and Range Province, Southwestern United States, for Isolation of High-Level Radioactive Waste—Basis of Characterization and Evaluation*. U.S. Geological Survey Professional Paper 1370-A. Washington, D.C.: U.S. Government Printing Office. ACC: NNA.19910524.0125.

BSC (Bechtel SAIC Company) 2002. *Guidelines for Developing and Documenting Alternative Conceptual Models, Model Abstractions, and Parameter Uncertainty in the Total System Performance Assessment for the License Application*. TDR-WIS-PA-000008 REV 00, ICN 01. Las Vegas, Nevada: Bechtel SAIC Company. ACC: MOL.20020904.0002.

BSC 2003a. *Site-Scale Saturated Zone Transport*. MDL-NBS-HS-000010 REV 01A. Las Vegas, Nevada: Bechtel SAIC Company. ACC: MOL.20030626.0180.

BSC 2003b. *SZ Flow and Transport Model Abstraction*. MDL-NBS-HS-000021 REV 00A. Las Vegas, Nevada: Bechtel SAIC Company. ACC: MOL.20030612.0138.

BSC 2003c. *Site-Scale Saturated Zone Transport*. MDL-NBS-HS-000010 REV 01B. Las Vegas, Nevada: Bechtel SAIC Company. ACC: MOL.20030919.0071.

Burbey, T.J. and Wheatcraft, S.W. 1986. *Tritium and Chlorine-36 Migration from a Nuclear Explosion Cavity*. DOE/NV/10384-09. Reno, Nevada: University of Nevada, Desert Research Institute, Water Resources Center. TIC: 201927.

CRWMS M&O (Civilian Radioactive Waste Management System Management and Operating Contractor) 2000. *Modeling Sub Gridblock Scale Dispersion in Three-Dimensional Heterogeneous Fractured Media (S0015)*. ANL-NBS-HS-000022 REV 00 ICN 01. Las Vegas, Nevada: CRWMS M&O. ACC: MOL.20001107.0376.

Gelhar, L.W. 1993. *Stochastic Subsurface Hydrology*. Englewood Cliffs, New Jersey: Prentice-Hall. TIC: 240652.

LANL (Los Alamos National Laboratory) 2003. *Software Code: FEHM*. V2.20. SUN, PC. 10086-2.20-00.

NRC (U.S. Nuclear Regulatory Commission) 2002. *Integrated Issue Resolution Status Report*. NUREG-1762. Washington, D.C.: U.S. Nuclear Regulatory Commission, Office of Nuclear Material Safety and Safeguards. TIC: 253064.

Painter, S.; Cvetkovic, V.; and Turner, D.R. 2001. "Effect of Heterogeneity on Radionuclide Retardation in the Alluvial Aquifer Near Yucca Mountain, Nevada." *Ground Water*, 39, (3), 326-338. Westerville, Ohio: National Ground Water Association. TIC: 254841.

Reamer, C.W. 2001. "U.S. Nuclear Regulatory Commission/U.S. Department of Energy Technical Exchange and Management Meeting on Total System Performance Assessment and Integration (August 6 through 10, 2001)." Letter from C.W. Reamer (NRC) to S. Brocoum (DOE/YMSCO), August 23, 2001, with enclosure. ACC: MOL.20011029.0281.

Reamer, C.W. and Williams, D.R. 2000. Summary Highlights of NRC/DOE Technical Exchange and Management Meeting on Radionuclide Transport. Meeting held December 5-7, 2000, Berkeley, California. Washington, D.C.: U.S. Nuclear Regulatory Commission. ACC: MOL.20010117.0063.

Sudicky, E.A. and Frind, E.O. 1982. "Contaminant Transport in Fractured Porous Media: Analytical Solutions for a System of Parallel Fractures." *Water Resources Research*, 18, (6), 1634-1642. Washington, D.C.: American Geophysical Union. TIC: 217475.

Zhang, D. 2002. *Stochastic Methods for Flow in Porous Media: Coping with Uncertainties*. San Diego, California: Academic Press. TIC: 254707.